CAMBRIDGE UNIVERSITY PRESS

New data on flatfish scuticociliatosis reveal that Miamiensis avidus and Philasterides dicentrarchi are different species

Journal:	*Parasitology*
Manuscript ID	PAR-2017-0052
Manuscript Type:	Research Article - Standard
Date Submitted by the Author:	01-Feb-2017
Complete List of Authors:	de Felipe, Ana; University of Santiago de Compostela, Microbiology and Parasitology Lamas, Jesús; University of Santiago de Compostela, Department of Cell Biology and Ecology Sueiro, Rosa; University of Santiago de Compostela, Microbiology and Parasitology Folgueira, Iria; Universidad de Santiago de Compostela, Instituto Análisis Alimentarios Leiro, Jose; Universidad de Santiago de Compostela, Instituto Análisis Alimentarios;
Key Words:	Paralichthys adspersus, Scophthalmus maximus, scuticociliates, SSUrRNA gene, α- β-tubulin gene

New data on flatfish scuticociliatosis reveal that *Miamiensis avidus* and *Philasterides dicentrarchi* are different species

ANA-PAULA DEFELIPE[1], JESÚS LAMAS[2], ROSA-ANA SUEIRO[1,2], IRIA FOLGUEIRA[1] and JOSÉ-MANUEL LEIRO [1*]

[1]*Departamento de Microbiología y Parasitología, Instituto de Investigación y Análisis Alimentarios, Universidad de Santiago de Compostela, 15782 Santiago de Compostela, Spain*

[2]*Departamento de Biología Celular y Ecología, Instituto de Acuicultura, Universidad de Santiago de Compostela, 15782 Santiago de Compostela, Spain*

SHORT TITLE: Scuticociliatosis in flatfish

[*]**Correspondence**

José M. Leiro, Laboratorio de Parasitología, Instituto de Investigación y Análisis Alimentarios, c/ Constantino Candeira s/n, 15782, Santiago de Compostela (A Coruña), Spain; Tel: 34981563100; Fax: 34881816070; E-mail: josemanuel.leiro@usc.es

SUMMARY

Scuticociliatosis is a severe disease in farmed flatfish. However, the causative agent is not always accurately identified. In this study, we identified two isolates of scuticociliates from an outbreak in cultured fine flounder *Paralichthys adspersus*. Scuticociliate identification was based on morphological data, examination of life stages and the use of molecular approaches. The isolates were compared with a strain of *Philasterides dicentrachi* from turbot *Scophthalmus maximus* and with a strain deposited in the American Type Culture Collection as *Miamiensis avidus* ATCC® 50180™. The use of morphological, biological, and molecular methods enabled us to identify the isolates from the fine flouder as *P. dicentrarchi*. Comparison of *P. dicentrachi* isolates and *M. avidus* revealed some differences in the buccal apparatus. Unlike *P. dicentrarchi, M. avidus* has a life cycle with three forms: macrostomes (capable of feeding on *P. dicentrarchi*), microstomes, and tomites. Additionally, we found differences in the 18S rRNA and α- and β-tubulin gene sequences, indicating that *P. dicentrarchi* and *M. avidus* are different species. We therefore reject the synonymy / conspecificity of the two taxa previously suggested. Finally, we suggest that a combination of morphological, biological, molecular (by multigene analysis), and serological techniques could improve the identification of scuticociliates parasites in fish.

Key words:

Paralichthys adspersus; *Scophthalmus maximus*; scuticociliates; SSUrRNA gene; α- β-tubulin gene.

INTRODUCTION

Scuticociliatosis is a parasitic disease caused by around 20 species of ciliates included in the subclass Scuticociliatia Small, 1967. The ciliates are common free-living members of limnetic and marine ecosystems and can transform into histiophagous parasites that cause serious infections in some aquatic animals (Kim *et al.* 2004a; Harikrishnan *et al.* 2010; Fan *et al.* 2011; Pan *et al.* 2013). Scuticociliates can infect a wide variety of teleost fish species: the European seabass *Dicentrarchus labrax* (Linnaeus, 1758) (Dragesco *et al.* 1995; Ramos *et al.* 2007); the Southern bluefin tuna *Thunnus maccoyii* (Castelnau, 1872) (Munday *et al.* 1997); the silver pomfret *Pampus argenteus* (Euphrasen, 1788) (Azad *et al.* 2007); the black rockfish *Sebastes schlegelii* Hilgendorf, 1880 (Whang *et al.* 2013); hatchery-reared juveniles of the Hapuku wreckfish *Polyprion oxygeneios* (Schneider & Forster, 1801) and adult kingfish *Seriola lalandi* Valenciennes, 1833 (Smith *et al.* 2009); the sea dragons *Phylloopteryx taeniolatus* (Lacepède, 1804) and *Phycodurus eques* (Günther, 1865) (Umehara *et al.* 2003; Rossteuscher *et al.* 2008; Bonar *et al.* 2013); the seahorses *Hippocampus erectus* Perry, 1810*, H. kuda* Bleeker,1852, *H. abdominalis* Lesson, 1872, and *H. hippocampus* (Linnaeus, 1758) (Thompson & Moewus 1964; Shin *et al.* 2011; di Cicco *et al.* 2013; Declercq *et al.* 2014; Ofelio *et al.* 2014); and elasmobranch fish such as the zebra shark *Stegostoma fasciatum* Hermann, 1783, the shark of Port Jackson *Heterodontus portusjacksoni* Meyer, 1793, and the Japanese bullhead shark *H. japonicus* Micklouho-MaClay and MacLeay, 1884 (Stidworthy *et al.* 2014). Scuticociliates also can colonize crustaceans and echinoderms, acting either as parasites or commensals (Small *et al.* 2005; Lynn & Strüder-Kypke 2005). One of the major problems in diagnosing fish scuticociliatosis is the difficulty in identifying the pathogenic species causing the disease. Although morphological and morphogenetic characters of the ciliary pattern

are routinely identified by using various silver impregnation methods, the systematic positions of certain taxa remain ambiguous and their characteristics must be reviewed so that species can be correctly identified (Jung *et al.* 2005; Miao *et al.* 2008; Gao *et al.* 2013). Biochemical, molecular, and immunological techniques must be accompanied by conventional morphological studies based on light microscopic analyses of live and silver-stained material for the correct identification of scuticociliate species, as well as for the reconstruction of the phylogenetic relationships and the analysis of the instraspecific variation between strains (Budiño *et al.* 2011a, 2012; Pan *et al.* 2013).

Many scuticociliates, especially species of the genera *Pseudocohnilembus* Evans and Thompson, 1964, *Uronema* Dujardin, 1841, *Miamiensis* Thompson and Moewus, 1964, and *Philasterides* Kahl, 1926, have been associated with infections in flatfish. Such infections seriously affect culture of the turbot *Scophthalmus maximus* (Linnaeus, 1758) and the olive flounder *Paralichthys olivaceus* (Temminck & Schlegel, 1846), causing high mortalities and economic losses on fish farms (Iglesias *et al.* 2001; Kim *et al.* 2004a). *Philasterides dicentrarchi* Dragesco, Dragesco, Coste, Gasc, Romestand, Raymond and Bouix, 1995 has been identified as the main aetiological agent of scuticociliatosis in farmed turbot and olive flounder on the basis of morphological and molecular criteria (Iglesias *et al.* 2001; Paramá *et al.* 2006; Kim *et al.* 2004a). Recently, Jung *et al.* (2005) identified several specimens isolated from the olive flounder as *Miamiensis avidus* Thompson & Moewus, 1964, on the basis of morphological criteria. Synonymy between these ciliate species was suggested after comparison of the morphological characteristics and the SSUrRNA gene sequences of *M. avidus* and *P. dicentrarchi* isolates (Jung *et al.* 2007). Hence, *P. dicentrarchi* is considered a junior synonym of *M. avidus* (Song & Wilbert 2000; Jung *et al.* 2007; Song *et al.* 2009a; Gao *et al.* 2010; Budiño *et al.* 2011a).

To date, identification and characterization of the species responsible for most outbreaks of scuticociliatosis in turbot and olive flounder have been based on the original morphological descriptions of *P. dicentrarchi* (Dragesco *et al.* 1995) and *M. avidus* (Thompson & Moewus, 1964), or on availabale data on nucleotide sequences of ribosomal genes obtained by different authors in various ciliate strains isolated from turbot (Paramá *et al.* 2006) and from olive flounder (Jung *et al.* 2011). However, identification has never been made by comparing the nucleotide sequences of the species *M. avidus* currently deposited in ATCC (*M. avidus* ATCC® 50180™). This restricts the accurate identification of this species at the molecular level.

In this study, we (i) describe an outbreak of scuticociliatosis in fine flounder *Paralichthys adspersus* (Steindachner, 1867) cultured in Peru and (ii) compare the morphological and biometrical characteristics, SSUrRNA, α– and β-tubulin gene sequences, antigenic relationships, tomitogenesis, and prey induced transformation in ciliates isolated from the fine flounder, in the ciliate *P. dicentrarchi* isolated from turbot, and in the ciliate species *M. avidus* ATCC® 50180™ (strain Ma/2). The results provide new data that should be considered in the identification of the aetiological agents of scuticociliatosis in flatfish.

MATERIAL AND METHODS

Animals and ethical approval

Twenty specimens of turbot *Scophpthalmus maximus* of approximately 50 g body weight were obtained from a local fish farm (Galicia, NW Spain). The fish were maintained in 50-l closed-circuit aerated tanks at 17-18 ºC. Ten ICR (Swiss) CD-1 mice (between eight and ten weeks old) initially supplied by the Charles River Laboratories (USA) were bred and maintained in the Central Animal Facility of the University of

Santiago de Compostela (Spain). The mice were held according to the criteria of protection, control, care and welfare of animals and the legislative requirements relating to the use of animals for experimentation (EU Directive 86/609 / EEC), the Declaration of Helsinki, and/or the Guide for the Care and Use of Laboratory Animals as adopted and promulgated by the US National Institutes of Health (NIH Publication No. 85-23, revised 1996). The Institutional Animal Care and Use Committee of the University of Santiago de Compostela approved all experimental protocols.

Isolation, ciliate culture, and experimental infections

In 2014, an outbreak of scuticociliatosis affecting the fine flounder *P. adspersus* was detected on a fish farm in Peru (Ancash, Huarmey Province). The farm was equipped with two water flow systems: one with closed and the other with open recirculation. Mortality was very high in both systems, affecting fish of different sizes. Outbreaks of scuticociliatosis in fine flounder coincided with a series of anomalies in the seawater temperature registered in the eastern Pacific region affected by El Niño resulting in an average temperature that was 3.1 ºC higher than the annual average (Comunicado Oficial ENFEN – Estudio Nacional del Fenómeno El Niño-Nº09-2014, Instituto del Mar del Perú –IMARPE). Ciliates were isolated from fish ranging from 16-27 cm in size (Fig. 1A). Two isolates of the scuticociliates, denominated Pe5 and Pe7, were obtained from ascitic fluid (with a concentration of approximately 5 x 10^6 trophozoites /ml) of naturally infected specimens of the fine flounder *P. adspersus*.

Virulent strain I1 of *P. dicentrarchi* was originally isolated from ascites fluid turbot from infected fish on a farm in Galicia (NW Spain) (Iglesias *et al.* 2001).

Strain Ma/2 of *M. avidus* deposited by A.T. Soldo and E. B. Small (Veterans Administration Medical Center, Miami, FL) with the name *Miamiensis avidus*

Thompson and Moewus (ATCC® 50180™) was acquired from the American Type Culture Collection (ATCC, USA). The strain Ma/2 of *M. avidus* belonged to the collection of Dr G.G. Holz and it was originally isolated by Dr L Moewus from infected seahorses and cultivated axenically since 1963 (Moewus, 1963; Kaneshiro *et al.* 1969).

Isolates Pe5, Pe7, and *P. dicentrarchi* strain I1 were maintained in the laboratory under the culture conditions described by Iglesias *et al.* (2003a). Strain Ma/2 of *M. avidus* was cultivated axenically in ATCC® medium 1651 MA (LGC Standards, Spain) at 25 ºC and subcultured every 3-5 days.

For experimental infections, turbot were injected intraperitoneally with 0.1 ml of 10^6 ciliates/ml (*M. avidus,* strain Ma/2) in phosphate-buffered saline (PBS) containing 10 mM Na_2HPO_4, 2mM KH_2PO_4, 2.7 mM KCl, and 137 mM NaCl, as previously described (Paramá *et al.* 2003), and the fish were observed daily for signs of infection and mortality. Infection was confirmed *post mortem* by the presence of ciliates in organs and tissues.

Morphological and histological analyses

Ciliates obtained at the exponential phase of culture (days 2-3) were concentrated by centrifugation at 700 *g* for 5 min and stained by a modification of the amoniacal silver carbonate method originally described by Fernández-Galiano (1994) and described in detail by Budiño *et al.* (2011a).

The nuclear apparatus was visualized by fluorescence, after staining ciliates with an aqueous solution of 0.4 µg/ml of 4'-6-diamidine-2-phenylindone (DAPI, Sigma-Aldrich), in a Zeiss Axioplan microscope (Jena, Germany) equipped with a DAPI filter set (BP 365/12; FT 395; LP 397) and in a Leica TCS SP2 laser scanning confocal microscope (Leica Biosystems, Mannheim, Germany).

Somatic and caudal cilia were measured in parasites fixed in 10% buffered formaldehyde under phase contrast optics.

In some experiments of prey-induction transformation, the ciliates were stained with the pH sensitive fluorescent acridine orange and observed in a fluorescence microscope with an excitation BP 450/490 nm dichroic mirror filter and FT 510 nm LP emission filter.

For histological study, tissues were fixed in 10% buffered formaldehyde solution, dehydrated through an ethanol series, embe dded in Paraplast Plus (Sigma-Aldrich), sectioned at 2-5 μm with a Leica RM 2135 rotary microtome (Leica Biosystems, Germany), and stained with haematoxylin and eosin (H&E) for examination by light microscopy (Iglesias *et al.* 2001).

Tomitogenesis and prey induction experiments

For tomite transformation, cultures of 2 x 10^3 cells/ml of *M. avidus* strain Ma/2, *P. dicentrarchi* strain I1 and isolate Pe5 in stationary phase were centrifuged at 700 *g* for 5 min, resuspended in non-nutrient synthetic seawater (NSS, 8 ‰ salinity), and incubated at 25 ºC (Gómez-Saladín & Small, 1993a). In prey induction experiments, ciliates of *M. avidus* strain Ma/2 and *P. dicentrachi* strain I1 were incubated at a ratio of 1:1 in 24-well microplates for 5 days in NSS at 25 ºC. The ciliates were observed daily under an inverted optical microscope. When predation phenomena were observed, ciliates were removed and centrifuged at 700 *g* for 5 min. Some specimens (10^6 ciliates) were fixed in buffered 10% formaldehyde in phosphate buffer saline for later examination by phase contrast microscopy, while other specimens (10^6 ciliates) were stained, using a modification of the ammoniacal silver carbonate method, as described previously.

PCR, cloning, and phylogenetic analyses

Cultured ciliates (5 x 10^6 cells/ml) were harvested by centrifugation at 700 *g* for 5 min. The ciliates were washed twice with phosphate buffer saline (PBS) and total DNA was purified with DNAeasy Blood and Tissue Kit (Qiagen) according to the manufacturer's instructions. DNA was analyzed to estimate its quality, purity, and concentration by an A_{260} measurement in a NanoDrop ND-1000 Spectrophotometer (NanoDrop Technologies, USA.). The DNA was stored at -20ºC until use.

PCR amplification was performed as previously described (Leiro *et al.* 2000; Budiño *et al.* 2011a), with minor modifications. A complete small-subunit ribosomal RNA (SSUrRNA; 1,759 bp), a region of 388 bp of the gene coding the β-tubulin, and a region of 197 bp of the gene coding the α-tubulin were amplified. The primer sets were designed and optimized by use of the Primer 3Plus program (http://www.bioinformatics.nl/cgi-bin/primer3plus/primer3plus.cgi), with default parameters. The PCR mixtures (25 µl) contained PCR reaction buffer (10 mM Tris-HCl, 50 mM KCl, 1.5 mM $MgCl_2$, pH 9.0), 0.2 mM of each deoxynucleoside triphosphate (dNTPs, Roche), 0.4 µM of each primer [forward 5'-AATCTGGTTGATCCTGCCAGT-3' / reverse 5'-GATCCTTCCGCAGGTTCA-3' (SSUrRNA); forward 5'-CCTACCACGGAGACTCTGATT-3' / reverse 5'-CCATAATTCTGTCGGGGTATT-3' (β-tubulin); forward 5'-ATGCCCTCTGATAAAACCATC-3' / reverse 5'-GAGTCCGGTACAGTTGTCAG-3' (α-tubulin)]; 0.5 units of high fidelity Taq polymerase (Nzyproof DNA polymerase; Nzytech, Portugal) and 50 ng of genomic DNA. The reactions were run in an automatic thermocycler (iCycler, BioRad, USA) as follows: initial denaturing at 94 ºC for 5 min, followed by 35 cycles at 94 ºC for 30 s, annealing at 55, 57, and 64 ºC (for SSUrRNA, α-tubulin and β-tubulin, respectively) for 45 s, and 72 ºC for 1 min; and finally a 7 min

extension phase at 72 ºC. The PCR products were analysed on a 4% agarose gel in tris acetate ethylenediaminetetraacetic acid (TAE) buffer (40 mMTris–acetate, pH 8.0, 2 mM EDTA) containing Sybr Green at 1x concentration (Intron, Korea), to verify the presence of bands of the correct size, and were photographed with a digital camera. The PCR products were cloned in the pSpark® II DNA cloning vector kit (Canvax Biotech, Spain) according to the manufacturer's instructions. After ligation of the PCR fragment, the *E. coli* $DH_{5\alpha}$ cells were transformed and then selected on the basis of antibiotic sensitivity and colour by culture on LB agar plates containing 100 µg/ml ampicillin, with 50 µl of a stock solution of 20 mg/ml of 5-bromo-4-chloro-3-indolyl-β-galactoside (X-Gal) and 20 µl of a 0.5 M solution of isopropylthio-β-D-galactoside (IPTG) spread on the surface. Ten *E. coli* white colonies per ligation sample were amplified in LB medium and plasmid DNA was purified with the QiAaprep® Spin Miniprep kit (Qiagen, Germany) according to the manufacturer's instructions. To confirm the presence of the cloned fragment of the correct size, the fragment was amplified by PCR, with the previously indicated primers and conditions. The PCR-amplified products were then visualized by agarose gel electrophoresis and sequenced in complementary directions (Sistemas Genómicos, Spain).

We used the BLAST interface and the blastn program optimized for very similar sequences (megablast), available at http://blast.ncbi.nlm.nih.gov , to calculate the degree of identity between the nucleotide sequences. Sequence alignment can be performed directly online.

The complete nucleotide sequences of the SSUrRNA gene from isolates Pe5 and Pe7 from fine flounder, strain I1 of *P. dicentrarchi* isolated from turbot, and strain Ma/2 of *M. avidus* (ATCC® 50180™) were compared with equivalent sequences from strains YK2 and YS2 of *M. avidus* isolated from olive flounder (accession numbers EU831208

and EU831200; Jung *et al*., 2011) and with other species of the order Philasterida (Table 1). The sequences were aligned with Clustal Omega (McWilliam *et al.,* 2013) and phylogenetic trees were inferred by the neighbour-joining (NJ) method (Saitou & Nei, 1987). This method was applied to the Kimura two-parameter correction model (Kimura, 1980) by bootstrapping with 1,000 replicates (Felsenstein, 1985) from multiple alignments and consensus of the study sequences with Clustal Omega software (Sievers *et al.* 2011). The tree is drawn to scale, with branch lengths in the same units as those of the evolutionary distances used to infer the phylogenetic tree. All positions containing gaps and missing data were eliminated and evolutionary analyses were conducted in MEGA7 (Kumar *et al.* 2016)

Production of recombinant alpha-tubulin (r-αTub) of P. dicentrarchi in yeast cells

RNA isolated from *Philasterides dicentrarchi* was purified with a NucleoSpin RNA kit (Macherey-Nagel, Düren, Germany) according to the manufacturer's instructions. After purification of the RNA, the quality, purity, and concentration were measured in a NanoDrop ND-1000 Spectrophotometer (NanoDrop Technologies, USA). The reaction mixture used for cDNA synthesis (25 µl/reaction mixture) contained 1.25 µM random hexamer primers (Promega), 250 µM of each deoxynucleoside triphosphate (dNTP), 10 mM dithiothreitol (DTT), 20 U of RNase inhibitor, 2.5 mM $MgCl_2$, 200 U of MMLV (Moloney murine leukemia virus reverse transcriptase; Promega) in 30 mM Tris and 20 mM KCl (pH 8.3), and 2 µg of sample RNA. The PCR was carried out with gene-specific primers designed from a partial sequence of the α-tubulin of *P. dicentrarchi* (forward/reverse primer pair 5'-AAAGAAGAAGGGGTACCTTTGGATAAAAGAatgccctctgataaaaccatc-3' / 5'-

TGGGACGCTCGACGGATCAGCGGCCGCTTAGTGGTGGTGGTGGTGGTGgagtc cggtacagttgtcag-3'). These primers were designed and optimized, using the *Saccharomyces* Genome Database (http://www.yeastgenome.org/). A hybridization region with the yeast YEpFLAG-1 (Eastman Kodak Company) plasmid and a poly His region (lower case letters correspond with the gene annealing zone) were included. The PCR reaction was initially developed at 95 °C for 5 min, and then for 30 cycles of 94 °C for 1 min, 53 °C for 1.5 min and 72 °C for 2 min. At the end of the 30 cycles, a 7-min extension phase was carried out at 72 °C. The PCR products were purified by using the Gene Jet PCR Purification Kit (Fermentas, Life Sciences) according to the manufacturer's instructions.

Purified PCR products were cloned in YEpFLAG-1 (Eastman Kodak Company) yeast expression vector, a plasmid carrying a TRP1 gene that completes the auxotrophy for the tryptophan for the host yeast (López-López *et al.* 2010).

Linearized plasmid YEpFLAG-1 was digested with *EcoRI* and *SalI* (Takara) and used to transform *Saccharomyces cerevisiae* cells (strain BJ 3505) by the lithium acetate procedure (Ito *et al.* 1983). The procedure involves co-transformation of yeast cells with the linearized empty plasmid and the PCR-generated DNA fragment, so that a recombination process occurs within the cell to yield a plasmid bearing the desired insert. Positive colonies were selected on complete medium containing glucose (20 g/l), but without tryptophan (CM-Trp), Yeast Nitrogen Base medium without amino acids (Sigma-Aldrich), except for the amino acids arginine, methionine and threonine at 10 mg/l; adenine, histidine, leucine, lysine, and tyrosine at 40 mg/l; and isoleucine and phenylalanine at 60 mg/l.

Plasmid DNA was then extracted with Easy Yeast Plasmid Isolation Kit (Clonetech) according to the manufacturer's instructions. The purified and cloned DNA fragment was subjected to sequencing analysis (Sistemas Genómicos, Spain).

Inoculation and polyclonal mouse antisera

CD-1 mice were inoculated i.p. with 200 µl of a 1:1 emulsion composed of 100 µl of a solution of 100 µg of r-αTub of the strain I1 of *P. dicentrarchi* in PBS and 100 µl of Freund complete adjuvant (Sigma-Aldrich). The same dose of r-αTub protein was prepared in Freund's incomplete adjuvant and injected i.p. in mice 15 and 30 days after the first immunization. The mice were bled via retrobulbar venous plexus seven days after the second inoculation. The blood was left to coagulate overnight at 4 ºC before the serum was separated by centrifugation (2000 *g* for 10 min), mixed 1:1 with glycerol, and stored at −20 ºC until use (Piazzon *et al.* 2011).

Immunoassays

For Western-blot assay, integral ciliate membrane-associate proteins (CMP) of scuticociliates were prepared as previously described (Iglesias *et al.* 2003b), with minor modifications (Mallo *et al.* 2013). Briefly, scuticociliate trophozoites were deciliated by the method described by Dickerson *et al.* (1989). The integral proteins were extracted by phase separation in Triton X-114 solution according to the method described by Bordier (1981). The proteins were precipited with cold acetone, and the precipitate was dried in a Speed Vac concentrator and stored at -80 ºC in 10 mM Tris-HCl, pH 7.5. Samples from CMP were separated under non-reducing conditions on linear SDS-PAGE 12.5 % gels (Piazzon *et al.* 2008). On completion of the electrophoresis, the gels were stained with Thermo Scientific GelCode Blue Safe Protein Stain (Thermo Fisher,

USA) for qualitative determination of the protein bands. At the same time, a gel was immunoblotted at 15 V for 35 min to Immobilon-P transfer membranes (0.45 μm; Millipore, USA) in a trans-blot SD transfer cell (Bio-Rad, USA) with transference buffer (48 mM Tris, 29 mM glycine, 0.037% SDS and 20% methanol, pH 9.2). The membrane was washed with Tris buffer saline (TBS; 50 mM Tris, 0.15 M NaCl, pH 7.4) and immediately stained with Ponceau S to verify transfer. After destaining the membrane with bidistilled water, a blocking solution consisting of TBS containing 0.2% Tween 20 and 3% BSA was added. The membrane was incubated for 1.5 h at room temperature and then washed in TBS and incubated overnight with the mouse polyclonal antisera anti-r-αTub (1:500 dilution) at 4 ºC. The membrane was washed again with TBS and incubated with rabbit anti-mouse IgG (Dakopatts; dilution 1:6000) for 1 h at room temperature. The membrane was then washed five times for 5 min with TBS and incubated for 1 min with enhanced luminol-based chemiluminiscent substrate (Pierce ECL Western Blotting Substrate, Thermo Scientific, USA), before finally being visualized and photographed with a FlourChem® FC2 imaging system (Alpha Innotech, USA).

The immunofluorescence assay was performed according to the previously described protocol (Mallo *et al.* 2015, 2016). Briefly, 5 x 10^6 ciliates were centrifuged at 750 *g* for 5 min, washed twice with Dulbecco's phosphate buffered saline (DPBS, Sigma Aldrich) and fixed for 5 min in a solution of 4% formaldehyde in DPBS. The ciliates were then washed twice with DPBS, resuspended in a solution containing 0.1% Triton X-100 (PBT) for 3 min and then washed twice with DPBS. They were then incubated with 1% bovine serum albumin (BSA) for 30 min. After this blocking step, the ciliates were incubated at 4 ºC overnight with a solution containing a 1:100 dilution of anti-r-αTub. The ciliates were then washed three times with DPBS and incubated, for

1 h at room temperature, with a 1:100 dilution of FITC conjugated rabbit/goat anti-mouse IgG-FITC antibody (Sigma) or with the same dilution of Alexa Fluor 546 conjugated goat anti-mouse Ig (Molecular Probes). After three washing steps in DPBS, the samples were double-stained with 0.8 mg/ml 4', 6-diamidine-2-phenylindole (DAPI; Sigma-Aldrich) in DPBS for 15 min at room temperature (Paramá *et al.* 2007). After another three washing steps in DPBS, the samples were mounted in PBS-glycerol (1:1) and visualized by fluorescence microscopy (Zeiss Axioplan, Germany) and/or confocal microscopy (Leica TCS-SP2, LEICA Microsystems Heidelberg GmbH, Mannheim, Germany).

The enzyme-linked immunosorbent assay (ELISA) was performed as previously described (Iglesias *et al.* 2003b), with minor modifications. One µg of CMP in 100 µl of carbonate-bicarbonate buffer (pH 9.6) was added to 96-well ELISA plates (high binding, Greiner Bio-One, Germany) and incubated overnight at 4 ºC. The wells were then washed three times with TBS and blocked for 1 h with TBS containing 0.2% Tween 20 (TBS-T_1) and 5% non-fat dry milk. The plates were incubated for 30 min at room temperature in a microplate shaker for ELISA (Stuart, UK) at 750 rpm with a 1:100 dilution (in TBS-T_1 containing 1% non-fat dry milk) of anti-r-αTub, and washed five times with TBS containing 0.05% Tween 20. Bound mouse antibodies were detected with a peroxidase-conjugated anti-mouse Ig polyclonal rabit serum (DAKO) diluted 1:1000 in TBS-T_1, and incubated for 30 min with shaking. The plates were washed five times in TBS, and 100 µl of *o*-phenylenediamine dihydrochloride (OPD, Sigma-Aldrich) and 0.003% H_2O_2 were added to each well. After incubation of the plates for 20 min at room temperature in darkness, the enzymatic reaction was stopped by adding 25 µl of H_2SO_4 at 3 N. Finally, the absorbance was read at 492 nm in a spectrophotometer microplate reader (Bio-Tek Instruments, USA).

Statistical analysis

Results are expressed as means ± standard error of means. Data were tested by one-way analysis of variance (ANOVA) followed by a Tukey-Kramer test for multiple comparisons. Differences were considered significant at $P < 0.05$.

RESULTS

Description of an outbreak of scuticociliatosis in the fine flounder Paralichthys adspersus

The outbreak of scuticociliatosis coincided with water temperatures higher than 21-22 ºC. The main external symptoms of the affected fish were alterations in skin pigmentation and emaciation (Fig. 1A), gills congested with mucus and abundant aneurysms (Fig. 1B, D), exophthalmia, and abdominal distension with ascitic fluid, from which ciliates were isolated (Fig. 1C). At the histopathological level, the main pathology was associated with systemic necrosis affecting several organs including the heart, with severe necrosis of myocardium (Fig. 1D).

Description of the Peruvian population (isolates Pe5 and Pe7) infecting the fine flounder P. adspersus (Fig. 2A-I; Table 2)

The main characteristics of the cilates isolated from the fine flounder are as follows: cells elongated and spindle-shaped, with a pointed anterior and rounded posterior end, a contractile vacuole, and a prominent caudal cilium (Fig. 2B, E, G, I, 3C). The buccal apparatus always contained two paroral membranes (PM1 and PM2) and three oral membranoids or polykinetids (M1, M2, and M3) (Fig. 2A, D, F, H),

showing identical morphology to that of *Philasterides dicentrarchi* (Fig. 2C). PM1 extends from the start of M1 to the start of M3, while PM2 extends from the middle of M3 to the end of the oral cavity (Fig. 2A, C, D, F, H). M1 is elliptical, M2 is trapezoidal, and M3 is smaller that M1 and M2, and irregularly triangular (Fig. 2A, C, D, F, H). The somatic ciliature of the Pe5 and Pe7 isolates consists of 10-13 kineties, and the pore of the subterminal contractile vacuole is at the posterior end of the second kinety (Fig. 2B, E, G, I).

The morphometric data of the Pe5 and Pe7 isolates are summarized in Table 2, in which they are compared with the morphometric data available for *P. dicentrarchi* isolated from turbot (strain I1; present study) and from seabass (Dragesco *et al.* 1995), and for *M. avidus* isolated from seahorses (Thompson & Moevus 1964) as well as with own data from of strain Ma/2 of *Miamiensis avidus* Thompson & Moewus (ATCC® 50180™) stained with ammoniacal silver carbonate and *P. dicentrachi* strain I1. The ranges of the morphological data on isolates Pe5 and Pe7 generally overlap those of *P. dicentrarchi* strain I1, of the original species description of *M. avidus,* and of *M. avidus* held by the ATCC. At the morphological level, isolates Pe5 and Pe7 and *P. dicentrarchi* strain I1 differ several morphological features from *M. avidus* (ATCC), such as the lack of a peak at the frontal part of trophozoites (Fig. 2M), the lack of a continuous paroral membrane (PM; Fig. 2J, K, L), and the morphology of the tomites, which are elongated and fusiforms in the latter species (Fig. 2N, O). In contrast to *M. avidus* (ATCC), the *P. adspersus* isolates Pe5 and Pe7 as well as *P. dicentrarchi* have a prominent caudal cilium that is longer than the somatic cilia (Fig. 3C). In *P. dicentrarchi,* the mean length of the caudal cilium was 11.4 ±2.0 μm (15 μm) and of the somatic cilia was 5.6 ± 1.0 μm (5-8 μm). In *M. avidus* strain Ma/2, the mean

length of the caudal cilium was 9.3 ± 2.1 μm (7-11 μm) and that of the somatic cilia, 6.6 ± 1.1 μm (5-9 μm, n=20).

The nuclear apparatus of isolates Pe5 and Pe7 and strain I1 of *P. dicentrarchi* consists of a spherical macronucleus located mainly in the middle or anterior third of the trophozoite, slightly lateralized, and between 4-8 μm in diameter (Table 2; Fig. 3A-C). The micronucleus, 1-2 μm in diameter, has a variable posterior position in isolates Pe5 and Pe7 and strain I1 of *P. dicentrarchi* (Fig. 3A-C), (Table 2). In *M. avidus* strain Ma/2, the macronucleus is irregularly spherical and usually located in the anterior cell half. The micronucleus anterior or laterally of the macronucleus (Fig. 3D).

Tomitogenesis and predatory transformation

Most polymorphic hymenostomes and scuticociliates have morphologically distinct feeding stages including a bacteriovorus microstome, a predatory macrostome, and sometimes a non-feeding, fast swimming tomite (Fig. 4). In culture media containing nutrients, *M. avidus* strain Ma/2 produced macrostome and microstome forms (Fig. 4A), wihile all strains of *P. dicentrarchi* only produced microstome forms (Fig. 4C). Under conditions of nutrient deprivation, *M. avidus* Ma/2 produced some macrostome and microstome forms and numerous tomites (Fig. 4B) *P. dicentrarchi* appeared almost exclusively as tomites (Fig. 4D). In *M. avidus* strain Ma/2, the macrostomes measured 50.1 ± 9.4 x 35.4 ± 5.2 μm (37-65 x 28-44 μm, n= 10) and the tomites 22.4 ±4.5 x 10.5 ±2.7 μm (23-28 x 7-13 μm, n= 10). In *P. dicentrarchi*, the length/width of the tomite was 20.6 ±2.7 x 13.1 ±2.1 (17-24 x 11-16 μm, n= 10).

To verify which of the species considered in this study developed predatory macrostome phases, we co-cultured trophozoites of *M. avidus* strain Ma/2 with trophozoites of *P. dicentrarchi* strain I1, and trophozoites of strain I1 with isolate Pe7,

in media without nutrients. On the second day, the co-cultures of *M. avidus* strain Ma/2 and *P. dicentrarchi* strain I1 showed predatory macrostome forms (Fig. 5A-D); however, this phenomenon was not detected in the co-cultures of Pe7 and I1 isolates. We found that *M. avidus* is a predator of *P. dicentrarchi* strain I1. To reach this conclusion, we obtained genomic DNA from *M. avidus* and *P. dicentrarchi* from 5 day co-cultures at day 5 and amplified it by PCR (Fig. 5E), using the primers designed for *P. dicentrarchi* DNA genes and showing low (α-tubulin), very low (β-tubulin) and high (SSUrRNA) nucleotide identity with the same genes in *M. avidus* (Fig. 5F). In all cases, we observed amplification of the SSUrRNA gene, slight amplification of the α-tubulin gene, and non-amplification of the β-tubulin gene in DNA samples obtained from cultures of the strain Ma/2 of *M. avidus* and in DNA samples from co-cultures of *M. avidus* and *P. dicentrarchi* (Fig. 5E, a-c). We then cloned and sequenced the amplified fragments of α-tubulin and SSUrRNA genes from co-cultures of *M. avidus* strain Ma/2 and *P. dicentrarchi* strain I1, observing that the nucleotide sequence obtained coincided with those of *M. avidus* Ma/2 (Fig. 5E, a, c).

Infectivity of M. avidus strain Ma/2

The *M. avidus strain* ATCC© 50180™ was originally isolated from infected seahorses; however, we did not know whether the species could infect flatfish. In this experiment, we inoculated turbot by intraperitoneal injection with *M. avidus,* using the same dose as used for *P. dicentrarchi* strain I1 (10^5 ciliates/fish). We observed that *M. avidus* strain Ma/2 is highly pathogenic to turbot, generating abdominal distension with a significant presence of ascitic liquid, from which it was possible to isolate ciliates (Fig. 6A), and causing 100% mortality in infected fish on day 5 (Fig. 6B).

Molecular analysis of the scuticociliates

The full length SSUrRNA sequences of Pe5, Pe7, and *P. dicentrarchi* strain I1 (Accession nº JX914665.1; Leiro *et al.* 2012, unpublished) showed 100% identity with each other and 96% identity with *M. avidus* strain Ma/2 (Accession KX357144; Table 3A). We compared the above- mentioned 18S sequences with those obtained from the GenBank for *M. avidus* isolate YK2 (Accession nº EU831208.1; Jung *et al.* 2011), *M. avidus* isolate YS2 (Accession EU831200.1; Jung *et al.* 2011), *M. avidus* isolate FXP2009050602 (Accession JN885091.1; Gao *et al.* 2012), and strain GF2008082801 of *Philasterides armatalis* Song, 2000 (Accession FJ848877; Gao *et al.* 2009). *Miamiensis avidus* strains YK2 and YS2 showed 99% identity with *P. dicentrachi* strain I1, Pe5 and Pe7 isolates, 96% identity with *M. avidus* strain Ma/2 or *M. avidus* isolate FXP2009050602, and 95% identity with *P. armatalis* (Table 3A). The phylogenetic tree constructed, using the Neighbour-joining (NJ) model grouped Pe5, Pe7, *P. dicentrachi* strain I1 in the same node and closely related to strains YK2, YS2 (Fig. 7A), while *M. avidus* strain Ma/2 from ATCC and the *M. avidus* isolate FXP2009050602 grouped in a different node together with the *Anophryoides haemophila* (Fig. **7**A). Analysis of the similarity between the nucleotide sequences corresponding to fragments of the α- (strain I1, accession KX357145; strain Ma/2, accession KX357143) and β-tubulin genes (strain I1, accession CQ342956.1; strain Ma/2 accession KX357147) revealed 99-100% identity between isolates Pe5, Pe7 and strain I1, but only 89% identity for α-tubulin and 85% identity for β-tubulin with *M. avidus* strain Ma/2 or 81-83% of identity for α-tubulin with *M. avidus* isolate FXP2009050602 (Table 3B). Phylogenetic trees generated after alignments of the nucleotide sequences of the α- and β-tubulin genes for the Pe5 and Pe7 isolates and I1 and the Ma/2 strains, using the model NJ, grouped Pe5,

Pe7 and I1 in one node and the *M. avidus* Ma/2 strain or isolate FXP2009050602 in a different node (Fig 7B, C).

Antigenic relationships between ciliates isolated from flatfish and M. avidus strain Ma/2

We generated a recombinant protein from a partial sequence of the gene encoding this protein (r-αTub) in *P. dicentrarchi* strain I1, to compare the antigenic homology between the α-tubulin of the scuticociliates Pe5, Pe7, I1, and *M. avidus* strain Ma/2 (ATCC® 50180™) (Fig. 8A). The antibodies generated in mice following inoculation with the recombinant protein were used to perform three immunoassays to determine the level of cross-reactivity with this protein in the isolates/strains studied.

We first performed an immunofluorescence test to verify the level of recognition by anti-r-αTub antibodies on the Pe5 andPe7 isolates and the I1 and Ma/2 strains. We found that the antibodies recognised the α-tubulins in all four samples and, at the concentrations used, we did not find any qualitative differences in the staining intensity (Fig. 8B-E).

Quantitative immunoassays as ELISA revealed that the levels of recognition of native ciliary proteins containing α-tubulin in the Pe7 isolate were similar to those obtained with strain I1; however, these levels were significantly lower when antigens of strain Ma/2 of *M. avidus* were used (Fig. 8F).

Western blot carried out under reducing conditions revealed two bands of about 50 and 60 kD in ciliary isolated fractions of isolate Pe7 and strain I1. However, no bands were detected when antigens from *M. avidus* strain Ma/2 were included (Fig. 8G).

DISCUSSION

Here we describe a scuticociliate infection in the fine flounder *Paralichthys adspersus,* cultivated in Peru. The infection occurred on a fish farm with a water recirculation system, which appears to increase the risk of scuticociliatosis (Budiño et al. 2011b), and at high temperatures, another risk factor for development of this disease (Iglesias *et al.* 2001; Moustafa *et al.* 2010).

We did not conduct a complete histopathological study of the scuticociliatosis in *P. adspersus* and only observed that the clinical signs and pathology generated by the ciliates are very similar to those produced in *Scophthalmus maximus* (Linnaeus, 1758) and the olive flounder *Paralichthys olivaceus* (Temminck & Schlegel, 1846) (Iglesias *et al.* 2001; Jung *et al.* 2007; Moustafa *et al.* 2010; Harikrishnan *et al.* 2012). Our research primarily focused on the identification of the causative agent of the disease in *P. adspersus*. In all samples, the buccal apparatus of the ciliate isolates Pe5 and Pe7 from *P. adspersus* contained two paroral membranes (PM1 and PM2) and three oral polykinetids (M1, M2 and M3), with identical arrangement and morphology to that described for *Philasterides dicentrarchi* (Dragesco *et al.* 1995; Iglesias *et al.* 2001; Budiño *et al.* 2011a). According to the redescription of the genus *Philasterides* Kahl, 1926 by Grolière (1980), the type species *Philasterides armata* has a split paroral membrane and three equidistant adoral poykinetids (M1, M2, and M3). However, of the two paroral membranes is debated as it is uncertain whther it respresent a fixed character that includes this species in the genus *Philasterides* or may show an intraspecific variability and is thus not suitable for species identification (Jung *et al.* 2007).

Song & Wilbert (2000) redescribed *M. avidus,* using the dimorphic paroral membrane with its monokinetidal anterior and its dikinetidal posterior part slightly

separated as its main morphological characteristic, thereby synonymizing *M. avidus* and *P. dicentrarchi*. However, the morphological data of the present study clearly shows that both isolates obtained from *P. adspersus* (isolates Pe5 and Pe7) have two clearly separated paroral membranes, while *M. avidus* strain Ma/2 has invariably a single continuous paroral membrane. The original description of *M. avidus* mentions that a narrow gap "sometimes" appears between the anterior and posterior paroral portions; however, this does not seem to be common in this species, as indicated by the fact that the authors described the paroral as a unit, measuring its length from its anterior to its posterior end until the anterior end (Thompson & Moewus, 1964). In contrast to *M. avidus,* the presence of a bipartite paroral membrane (PM1 and PM2), seems thus to be a constant morphological feature in *P. dicentrarchi* (Dragesco *et al.* 1995; Iglesias *et al.* 2001; Budiño *et al.* 2011a).

Jung *et al.* (2007) found that a scuticociliate isolate (YS1 strain) from olive flounder, identified as *M. avidus*, has one or two paroral membranes and two or three oral polykinetids, the authors concluded that the morphology of buccal structures "cannot be used as a consistent key for identification of the species*"*. However variability reported by Jung *et al.* (2007), might the result of a stomatogenic sequence in the organelles membranoidogenesis, which is very common in several species of scuticociliates (Miao et al. 2010). Some studies clearly show that *M. avidus* has a continuous paroral membrane; only in the first phases of stomatogenesis (during the transformation of microstomes into to macrostomes), the paroral membrane is divided, with a small segment at the posterior end (Gómez-Saladín & Small, 1993a).

The morphology of oral polykinetids M1, M2, and M3 in isolates Pe5 and Pe7 and *Philasterides dicentrarchi* strain I1 is very similar to that observed in *M. avidus*; but differs from the oral polykinetids of congeners. the M1 of isolates Pe5 and Pe7 and

570 strain I1 of *P. dicentrarchi* is elongated like the M1 of *M. avidus* (Thompson &
571 Moewus, 1964), while the M1 of *P. armata* and *P. armatalis* is usually triangular
572 (Grolière 1980; Song *et al.* 2000); the M3 in *P. dicentrarchi* strain I1 and in the isolates
573 Pe5 and Pe7 is irregularly triangular and similar to *M. avidus* (Thompson & Moewus,
574 1964), but different from the rectangular M3 of *P. armata* (Grolière, 1980).

575 During early and late phases of equal fission, most ciliates share certain features,
576 such as common position of macronucleus and micronucleus, synchronization of
577 macronuclear amitosis and fission furrow, and a specific and well defined dividing size
578 (Long & Zufall, 2010). The position of the micronucleus relative to the macronucleus is
579 not specified in the original descriptions of *P. dicentrarchi* and *M. avidus*, which only
580 states that the micronucleus is closely associated with the macronucleus but completely
581 separate from it in *P. dicentrarchi* (Dragesco *et al.* 1995; Paramá *et al.* 2006); however,
582 some later descriptions proposed the anterior position of the micronucleus relative to the
583 macronucleus as a specific characteristic of *M. avidus* (Hu *et al.* 2009). In this study, we
584 clearly demonstrate that the position of the micronucleus relative to the macronucleus in
585 Pe5, Pe7 isolates and in strain I1 of *P. dicentarchi* is very variable.

586 The formation of tomites, which is a general characteristic of scuticociliates,
587 occurs in response to starvation without cyst production, or in response to drugs
588 (Fenchel, 1987; Gómez-Saladín & Small, 1993b, Morais *et al.* 2009). *Miamiensis*
589 *avidus* is a known tomite-producing scuticociliate (Thompson & Moewus, 1964;
590 Gómez-Saladin & Small, 1993a; b). The life cycles of scuticociliates provide further
591 taxonomically significant features. While *M. avidus* undergoes microstome to
592 macrostome transformation following a considerable change in cell size and the buccal
593 structures (Small, 1967; Gómez-Saladin & Small, 1993a), such a transformation was
594 not observed in *P. dicentrarchi* (Dragesco *et al.* 1995). In the present study, we

performed tomitogenesis and prey-induced transformation experiments with *M. avidus* strain Ma/2, *P. dicentrarchi* strain I1 isolated from *P. adspersus,* and isolate Pe7 in a nutrient-depleted medium. We observed induction of the macrostome forms only in *M. avidus* strain Ma/2*,* and in co-cultures of this strain Ma/2 with the *P. dicentrarchi* strain I1; however, this phenomenon does not occur when I1 trophozoites were incubated with trophozoites of isolates (Pe7) of fine flounder, and neither macrostome forms nor any sign of predation/cannibalism could be detected.

The scuticociliate isolates Pe5 and Pe7 from the fine flounder *P. adspersus* and *P. dicentrarchi* strain I1 are obviously virulent in their hosts; however, the infective capacity of the *M. avidus* strain Ma/2, which has been maintained in culture for a long time (more than 40 years) in the ATCC collection (Soldo & Merlin, 1972), in unknown In the present study, we demonstrated the high virulence of the strain Ma/2, causing a mortality of 100% in turbot after experimental infection.

Identification of scuticociliates only on the basis of morphological features may lead to misidentification (Whang *et al.* 2013). To solve this problem, molecular techniques, mainly on the analysis of the small subunit rRNA gene (SSUrRNA) are used. Besides barcoding for identification, they also enable clarification of the phylogenetic relationships and the taxonomy of scuticociliates (Gao *et al.* 2012). The phylogenetic analysis reveal a cluster of *P. dicentrarchi* strains I1 and isolates Pe7 and Pe5 as sister group of strains YK2 and YS2, which from olive flounder, that had been identified as *M. avidus* (syn. *P. dicentrarchi*) (Song & Wilbert, 2000; Jung *et al.* 2007) and whose SSUrRNA gene sequence data have been described in previous studies by Jung *et al.* (2005) and Song *et al.* (2009a; b). *Miamiensis avidus* strain Ma/2, which is considered to represent the “real” *M. avidus* and the isolate FXP2009050602, a strain that is very morphologically similar to *M. avidus* described by Song & Wilbert (2000),

but differs in some morphological characteristics, and shows great differences at the molecular level with the strains from Korea (Jung *et al.* 2011; Gao *et al.* 2012), together and both are related to *Anoprhyoides haemophila,* a species that has already been included with *M. avidus* in the family Parauronematidae on the basis of SSUrRNA topologies (Gao *et al.* 2012). These results therefore indicate that the Peruvian isolates from *P. adspersus* are similar to *P. dicentrarchi* and closely related to strains YK2 and YS2; however, they are phylogenetically most distant from strain Ma/2 and isolate FXP2009050602 of *M. avidus*. To corroborate this, we compared the α/β tubulin gene sequences in *P. dicentrarchi* and *M. avidus* strain Ma/2 held in the ATCC and isolate FXP2009050602 of *M. avidus* provide valuable information about the taxonomic position of the species analyzed (Stoeck *et al.* 2000; Schmidt *et al.* 2006; Barth *et al.* 2006; Budiño *et al.* 2011a). α– and β-tubulin genes are suitable phylogenetic markers discriminating strains and investigat the intraspecific genetic variability in *P. dicentrarchi* (Budiño et al. 2011a). The nucleotide sequences identity of 99% and 100%, respectively in the α- and β-tubulin genes, indicate a conspecificity. The differences between the *P. dicentrarchi* strains and *M. avidus* strain Ma/2 were also confirmed at serological level. Although serological tests are widely used for identification in other protozoa (de Waal, 2012), they are not usually used to diagnose ciliate infections in fish. Nonetheless, they have proved very useful for characterizing and distinguishing antigens from *P. dicentrarchi* and *M. avidus*, expressed during infection in turbot and in olive flounder, and thus to differentiate strains (Piazzon *et al.* 2008; Song *et al.* 2009b; Budiño *et al.* 2012). These findings confirm the above-mentioned genetic findings on comparing the nucleotide sequences of the gene encoding this protein.

Final conclusion. The morphological analysis, tomitogenesis and prey-induced transformation, comparisons of SSUrRNA and α/β tubulin gene sequences, and

serological analysis all clearly indicate that isolates Pe5 and Pe7 and *P. dicentrarchi* strain I1 are not conspecific with *M. avidus* strain Ma/2 (ATCC). We also found that *P. dicentrarchi* displayed low identity in SSUrRNA sequences with *P. armatalis*. The low identity (based on the nucleotide sequences of this gene) between *P. dicentrarchi* and *P. armatalis* was also described by Gao *et al.* (2012).

Until the nucleotide sequences of the 18S gene of the type species *P. armatalis* becomes available, we cannot definitely confirm that this species belongs to the genus *Philasterides*, or whether it should be transferred to another genus, or even propose its inclusion in a new genus.

The analysis of SSUrRNA gene sequences indicates that *P. dicentrarchi* obtained from turbot and fine flounder (I1, Pe5 and Pe7) and isolates YK2 and YS2 from olive flounder of *Miamiensis avidus* are the same ciliate species, suggesting that the latter have been misidentified. Morphological analysis of all of these isolates is therefore urgently required for their correct identification.

In conclusion, the aetiological agent of scuticociliatosis produced in the fine flounder *Paralichthys adspersus* is the same as that described in the olive flounder *Paralichthys.olivaceus* and the turbot *S. maximus*. Due to the lack of information regarding the nucleotide sequence of the SSUrRNA gene in the type species of *Philasterides,* we suggest that the name *P. dicentrarchi* should be maintained for the species that causes scuticociliatosis in turbot and fine flounder.

ACKNOWLEDGEMENTS

We are grateful for the support provided by Jaime Pauro (Headship of Pacific Aquaculture Deep Frozen S A-Perú-) and by Dr Violeta Flores and Marco Medina of the IMERPA (Peru) for technical assistance with scuticociliate isolation. This study was

financially supported by grant AGL2014-57125-R from the Ministerio de Economía y Competitividad (Spain), by grant GPC2014/069 from the Xunta de Galicia (Spain) and by PARAFISHCONTROL project. This project received funding from the *European Union's Horizon 2020 research and innovation programme* under grant agreement No. 634429. This publication reflects the views only of the authors, and the European Commission cannot be held responsible for any use, which may be made of the information contained therein.

REFERENCES

Azad, I.S., Al-Marzouk, A., James, C.M., Almatar, S. and Al-Gharabally, H. (2007). Scuticociliatosis-associated mortalities and histopathology of natural infection in cultured silver pomfret (*Pampus argenteus* Euphrasen) in Kuwait. *Aquaculture* **262**, 202–210.

Bart, D., Drenek, S., Fokin, S. and Berendonk, T.U. (2006). Intraspecific genetic variation in *Paramecium* revealed by mitochondrial cytochrome c oxidase I sequences. *Journal of Eukaryotic Microbiology* **53**, 20-25.

Bonar, C.J., Garner, M.M., Weber, E.S., Keller, C.J., Murray, M., Adams, L.M.a and Frasca S. Jr. (2013). Pathologic findings in weedy (*Phyllopteryx taeniolatus*) and leafy (*Phycodurus eques*) seadragons. *Veterinary Pathology* **50**, 368-376.

Bordier, C. (1981). Phase separation of integral membrane proteins in Triton X-114. *The Journal of Biological Chemistry*, **256**,1604-1607.

Budiño, B., Lamas, J., Pata, M.P., Arranz, J.A., Sanmartín, M.L. and Leiro, J. (2011a). Intraspecific variability in several isolates of *Philasterides dicentrarchi*

(syn. *Miamiensis avidus*), a scuticociliate parasite of farmed turbot. *Veterinary Parasitology* **175**, 260-272.

Budiño, B., Lamas, J., González, A., Pata, M.P., Devesa, S., Arranz, J.A. and Leiro, J. (2011b). Coexistence of several *Philasterides dicentrarchi* strains on a turbot fish farm. *Aquaculture* **322-323**, 23-32.

Budiño, B., Leiro, J., Cabaleiro, S. and Lamas, J. (2012). Characterization of *Philasterides dicentrarchi* isolates that are pathogenic to turbot: serology and cross-protective immunity. *Aquaculture*, **364-365**, 130-136.

de Waal, T. (2012). Advances in diagnosis of protozoan diseases. *Veterinary Parasitology* **189**, 65-74.

Declercq, A.M., Chiers, K., Van den Broeck, W., Rekecki, A., Teerlinck, S., Adriaens, D., Haesebrouck, F. and Decostere, A. (2014). White necrotic tail tips in estuary seahorses, *Hippocampus kuda*, Bleeker. *Journal of Fish Diseases* **37**, 501-504.

di Cicco, E., Paradis, E., Stephen, C., Turba, M.E. and Rossi, G. (2013). Scuticociliatid ciliate outbreak in Australian potbellied sea horse, *Hippocampus abdominalis* (Lesson, 1827): clinical signs, histopathological findings, and treatment with metronidazole. *Journal of Zoo and Wildlife Medicine* **44**, 435-440.

Dickerson, H.W., Clark, T.G. and Findly, R.C. (1989). *Ichthyophthirius multifiliis* has membrane-associated immobilization antigens. *The Journal of Protozoology* **36**, 159-164.

Dragesco, A., Dragesco, J., Coste, F., Gasc, C., Romestand, B., Raymond, J. and Bouix, G. (1995). *Philasterides dicentrarchi,* n. Sp. (Ciliophora, Scuticociliatida), a histiophagous opportunistic parasite of *Dicentrarchus labrax*

(Linnaeus, 1758), a reared marine fish. *European Journal of Protistology* **31**, 327-340.

Fan, X., Hu, X., Al-Farraj, S.A., Clamp, J.C. and Song W. (2011). Morphological description of three marine ciliates (Ciliophora, Scuticociliatia), with establishment of a new genus and two species. *European Journal of Protistology* **47**, 186-196.

Felsenstein, J. (1985). Confidence limits on phylogenies: and approach using the boostrap. *Evolution* **39**, 783-791.

Fenchel, T. (1987). Adaptative significance of polymorphic life cycles in protozoa: resposes to starvation and reffeding in two species of marine ciliates. *Journal of Experimental Marine Biology and Ecology* **136**, 159-177.

Fernández-Galiano, D. (1994). The ammoniacal silver carbonate method as a general procedure in the study of protozoa from sewage (and other) waters. *Water Research* **28**, 495-496.

Gao, F., Fan, X., Yi, Z., Strüder-Kypke, M. and Song, W. (2010). Phylogenetic consideration of two scuticociliate genera, *Philasterides* and *Boveria* (Protozoa, Ciliophora) based on 18 S rRNA gene sequences. *Parasitology International* **59**, 549-555.

Gao, F., Katz, L.A. and Song W. (2012). Insights into the phylogenetic and taxonomy of philasterid ciliates (Protozoa, Ciliophora, Scuticociliatia) based on analyses of multiple molecular marker. *Molecular Phylogenetics and Evolution* **64**, 308-317.

Gao, F., Katz, L.A. and Song, W. (2013). Multigene-based analyses on evolutionary phylogeny of two controversial ciliate orders: Pleuronematida and Loxocephalida (Protista, Ciliophora, Oligohymenophorea). *Molecular Phylogenetics and Evolution* **68**, 55-63.

Gómez-Saladín, E. and Small, E.B. (1993a). Oral morphogenesis of the microstome to macrostome transformation in *Miamiensis avidus* strain Ma/2. *Journal of Eukaryotic Microbiology* **40**, 363-370.

Gómez-Saladin, E. and Small, E.B. (1993b). Starvation induces tomitogenesis in *Miamiensis avidus* strain Ma/2. *Journal of Eukaryotic Microbiology* **40**, 727-730.

Grolière, C.A. (1980). Morphologie et stomatogenèse chez deux ciliés Scuticociliatida des genres *Phïlasterides* Kahl, 1926 et *Cyclidium* O. F. Müller; 1786. *Acta Protozoologica* **19**, 195-206.

Harikrishnan, R., Balasundaram, C. and Heo, M.S. (2010). Scuticociliatosis and its recent prophylactic measures in aquaculture with special reference to South Korea Taxonomy, diversity and diagnosis of scuticociliatosis: Part I Control strategies of scuticociliatosis: Part II. *Fish and Shellfish Immunology* **29**, 15-31.

Harikrishnan, R., Jin, C.N., Kim, J.S., Balasundaram, C. and Heo, M.S. (2012). *Philasterides dicentrarchi*, a histophagous ciliate causing scuticociliatosis in olive flounder, *Philasterides dicentrarchi* –Histopathology investigations. *Experimental Parasitology* **130**, 239-245.

Hu, X., Song, W. and Warren, A. (2009). Scuticociliatids. In. Free-living Ciliates in Bohai and Yellow Sea, China. (Song W., Warren A. & Hu X. ,eds.) Science Press. Beijing.

Iglesias, R., Paramá, A., Álvarez, M.F., Leiro, J., Fernández, J. and Sanmartín, M.L. (2001). *Philasterides dicentrarchi* (Ciliophora, Scuticociliatida) as the causative agent of scuticociliatosis in farmed turbot, *Scophthalmus maximus* in Galicia (NW Spain). *Diseses of Aquatic Organisms* **46**, 47-55.

766 **Iglesias, R., Paramá, A., Álvarez, M.F., Leiro, J., Aja, C. and Sanmartín, M.L.**
767 (2003a). *In vitro* growth requeriments for the fish pathogen *Philasterides*
768 *dicentrarchi* (Ciliophora, Scuticociliatida). *Veterinary Parasitology* **111**, 19-30.
769 **Iglesias, R., Paramá, A., Álvarez, M.F., Leiro, J., Ubeira, F.M. and Sanmartín,**
770 **M.L.** (2003b). *Philasterides dicentrarchi* (Ciliophora: Scuticociliatida) express
771 surface immobilization antigens that probably induce protective immune
772 responses in turbot. *Parasitology* **126**, 125-134.
773 **Ito, H., Fukuda, Y., Murata, K. and Kimura, A.** (1983). Transformation of intact
774 yeast cells treated with alkali cations. *Journal of Bacteriology* **153**, 163–168.
775 **Jung, S.J., Kitamura, S.I., Song, J.Y., Joung, I.Y. and Oh, M.J.** (2005). Complete
776 small subunit rRNA gene sequence of the scuticociliate *Miamiensis*
777 *avidus* pathogenic to olive flounder *Paralichthys olivaceus*. *Diseases of Aquatic*
778 *Organisms* **64**, 159–162.
779 **Jung, S.J., Kitamura, S.I., Song, J.Y. and Oh, M.J.** (2007). *Miamiensis avidus*
780 (Ciliophora: Scuticociliatida) causes systemic infection of olive flounder
781 *Paralichthys olivaceus* and is a senior synonym of *Philasterides dicentrarchi*.
782 *Diseases of Aquatic Organisms* **73**, 227-234.
783 **Jung, S.J., Im, E.Y., Struder-Kypke, M.C., Kitamura, S. and Woo, P.T.** (2011).
784 Small subunit ribosomal RNA and mitochondrial cytochrome c oxidase subunit
785 1 gene sequences of 21 strains of the parasitic scuticociliate *Miamiensis avidus*
786 (Ciliophora, Scuticociliatia). *Parasitology Research* **108**, 1153-1161.
787 **Kim, S.M., Cho, J.B., Kim, S.K., Nam, Y.K. and Kim, K.H.** (2004a). Occurrence of
788 scuticociliatosis in olive flounder *Paralichthys olivaceus* by *Philasterides*
789 *dicentrarchi* (Ciliophora: scuticociliatia). *Diseases of Aquatic Organisms* **62**,
790 2333-2338..

Kaneshiro, E.S., Dunham, P.B. and Holz, G.G. (1969). Osmorregulation in a marine ciliate, *Miamiensis avidus*. I. Regulation of inorganic ions and water. *The Biological Bulletin* **136**, 65-75.

Kimura, M. (1980). A simple method for estimating evolutionary rates of base substitutions through comparative studies of nucleotide sequences. *Journal of Molecular Evolution* **16**, 111-120.

Kumar, S., Stecher, G., and Tamura, K. (2016). MEGA7: Molecular Evolutionary Genetics Analysis version 7.0 for bigger datasets. *Molecular Biology and Evolution* **33**: 1870-1873.

Leiro, J., Siso, M.I., Paramá, A., Ubeira, F.M. and Sanmartín, M.L. (2000). RFLP analysis of PCR-amplified small subunit ribosomal DNA of three fish microsporidian species. *Parasitology* **124**, 145-151.

Long, H. and Zufall, R.A. (2010). Diverse modes of reproduction in the marine free-living ciliate *Glauconema trihymene*. *BioMed Central Microbiology* **10**, 108.

López-López, O., Fuciños, P., Pastrana, L., Rúa, M.L., Cerdán, M.E. and González-Siso, M.I. (2010). Heterologous expression of an esterase from *Thermus thermophilus* HB27 in *Saccharomyces cerevisiae*. *Journal of Biotechnology* **145**, 226-232.

Ly**nn, D.H. and Strüder-Kypke, M.** (2005). Scuticociliate endosymbionts of echinoids (phylum Echinodermata): phylogenetic relationships among species in the genera *Entodiscus, Plagiopyliella, Thyrophylax,* and *Entorhipidium* (phylum Ciliophora). *The Journal of Parasitology* **91**, 1190-1199.

McWilliam, H., Li, W., Uludag, M., Squizzato, S., Park, Y.M., Buso, N., Cowley, A.P., and López, R. (2013). Analysis tool web services from the EMBL-EBI. *Nucleic Acids Research* **41**(Web Server issue), W597-W600.

Mallo, N., Lamas, J. and Leiro, J.M. (2013). Evidence of an alternative oxidase pathway for mitochondrial respiration in the scuticociliate *Philasterides dicentrarchi*. *Protist* **164**, 824-836.

Mallo, N., Lamas, J., Piazzon, C. and Leiro, J.M. (2015). Presence of a plant-like proton-translocating pyrophosphatase in a scuticociliate parasite and its role as a possible drug target. *Parasitology* **142**, 449-462.

Mallo, N., Lamas, J., Defelipe, A.P., Decastro, M.E., Sueiro, R.A. and Leiro, J.M. (2016). Presence of an isoform of H+-pyrophosphatase located in the alveolar sacs of a scuticociliate parasite of turbot: physiological consequences. *Parasitology* **143**, 576-587.

Mi**ao, M., Warren, A., Song, W., Wang, S., Shang, H. and Chen, Z.** (2008). Analysis of internal transcribed spacer 2 (ITS2) region of scuticociliates and related taxa (Ciliophora, Oligohymenophorea) to infer their evolution and phylogeny. *Protist* **159**, 519-533.

Miao, M., Wang, Y., Song, W., Clamp, J. C., and Al-Rasheid, K. A. S. (2010). Description of *Eurystomatella sinica* n. gen., n. sp., with establishment of a new family Eurystomatellidae n. fam. (Protista, Ciliophora, Scuticociliatia) and analyses of its phylogeny inferred from sequences of the small-subunit rRNA gene. *International Journal of Systematic and Evolutionary Microbiology* **60**, 460-468

Moewus, L. (1963). Studies on a marine parasitic ciliate as a potential virus vector. In: Symp. on Marine Microbiology. pp. 366-379. C.H. Oppenheimer (Ed.), Charles C. Thomas, Springfield, Ill.

Morais, P., Lamas, J., Sanmartín, M.L., Orallo, F. and Leiro, J. (2009). Resveratrol induces mitochondrial alterations, autophagy and a cryptobiosis-like state in scuticociliates. *Protist* **160**, 552-564.

Moustafa, E.M.M., Naota, M., Morita, T., Tange, N. and Shimada, A. (2010). Pathological study on the scuticociliatosis affecting farmed Japanese flounder (*Paralichthys olivaceus*) in Japan. *The Journal of Veterinary Medical Science* **72**, 1359-1362.

Munday, B.L., O'Donoghue, P.J., Watts, M., Rough, K. and Hawkesford, T. (1997). Fatal encephalitis due to the scuticociliate *Uronema nigricans* in sea-caged, southern bluefin tuna *Thunnus maccoyii*. *Diseases of Aquatic Organisms* **30**, 17-25.

Ofelio, C., Blanco, A., Roura, A., Pintado, J., Pascual, S. and Planas, M. (2014). Isolation and molecular identification of the scuticociliate *Porpostoma notata* Moebius, 1888 from moribund reared *Hippocampus hippocampus* (L.) seahorses, by amplification of the SSU rRNA gene sequences. *Journal of Fish Diseases* **37**, 1061-1065.

Pan, X., Zhu, M., Ma, H., Al-Rasheid, K.A. and Hu, X. (2013). Morphology and small-subunit rRNA gene sequences of two novel marine ciliates, *Metanophrys orientalis* spec. nov. and *Uronemella sinensis* spec. nov. (Protista, Ciliophora, Scuticociliatia), with an improved diagnosis of the genus *Uronemella*. *International Journal of Systematic and Evolutionary Microbiology* **63**, 3515-23.

Paramá, A., Iglesias, R., Álvarez, M.F., Leiro, J., Aja, C. and Sanmartín, M.L. (2003). *Philasterides dicentrarchi* (Ciliophora, Scuticociliatida): experimental infection and posible routes of entry in farmed turbot *(Scophthalmus maximus*). *Aquaculture* **217**, 73-80.

Paramá, A., Arranz, J.A., Álvarez, M.F., Sanmartín, M.L. and Leiro, J. (2006). Ultrastructure and phylogeny of *Philasterides dicentrarchi* (Ciliophora: Scuticociliatia) from farmed turbot in NW Spain. *Parasitology* **132**, 555-564.

Paramá, A., Castro, R., Lamas, J., Sanmartín, M.L., Santamarina, M.T., and Leiro, J. (2007). Scuticociliate proteinases may modulate turbot immune response by inducing apoptosis in pronephric leucocytes. *International Journal for Parasitology* **37**, 87-95.

Piazzon, C., Lamas, J., Castro, R., Budiño, B., Cabaleiro, S., Sanmartín, M.L., and Leiro, J. (2008). Antigenic and cross-protection studies on two turbot scuticociliate isolates. *Fish and Shellfish Immunology* **25**, 417-424.

Piazzon, C., Lamas, J. and Leiro, J.M. (2011). Role of scuticociliate proteinases in infection success in turbot, *Psetta maxima* (L.). *Parasite Immunology* **33**, 535-544.

Ramos, M.F., Costa, A.R., Barandela, T., Saraiva, A. and Rodrigues, P.N. (2007). Scuticociliate infection and pathology in cultured turbot *Scophthalmus maximus* from the north of Portugal. *Diseases of Aquatic Organisms* **74**, 249-253.

Rossteucher, S., Wenker, C., Jermann, T., Wahli, T., Oldenberg, E. and Schmidt-Posthaus, H. (2008). Severe scuticociliate (*Philasterides dicentrarchi*) infection in a population of sea dragons (*Phycodurus eques* and *Phylopteryx taeniolatus*). *Veterinary Parasitology* **45**, 546-550.

Schmidt, S.L., Benhart, D., Schlegel, M. and Fried, J. (2006). Fluorescence *in situ* with specific oligonucleotide rRNA probes distinguishes the sibling species *Stylonychia lemnaea* and *Stylonychia mytilus* (Ciliophora, Spirotrichea). *Protist* **157**, 21-30.

888 **Shin, P.S., Han, J.E., Gómez, D.K., Kim, J.H., Choresca, Jr. C.H., Jun, J.W., and**
889 **Park, S.C.** (2011). Identification of scuticociliate *Philasterides dicentrarchi*
890 from indo-pacific seahorses *Hippocampus kuda. African Journal of*
891 *Microbiology Research* **5**, 738-741.
892 **Sievers, F., Wilm, A., Dineen, D., Gibson, T.J., Karplus, K., Li, W., López,**
893 **R., McWilliam, H., Remmert, M., Söding, J., Thompson, J.D. and Higgins,**
894 **D.G.** (2011). Fast, scalable generation of high-quality protein multiple sequence
895 alignments using Clustal Omega. *Molecular Systems Biology* **7**, 539.
896 **Saitou, N. and Nei M.** (1987). The neighbor-joining method: A new method for
897 reconstructing phylogenetic trees. *Molecular Biology and Evolution* **4**, 406-425.
898 **Small, E.B.** (1967). The scuticociliatida, a new Order onf the Class Ciliatea (Phylum
899 Protozoa, Subphylum Ciliophora). *Transactions of the American Microscopical*
900 *Society* **86**, 345-370.
901 **Small, H.J., Neil, D.M., Taylor, A.C., Bateman, K. and Coombs, G.H.** (2005). A
902 parasitic scuticociliate infection in the Norway lobster (*Nephrops norvegicus*).
903 *Journal of Invertebrate Pathology* **90**, 108-117.
904 **Smith, P.J., McVeagh, S.M., Hulston, D., Anderson, S.A. and Gublin, Y.** (2009).
905 DNA identification of ciliates associated with disease outbreaks in a New
906 Zealand marine fish hatchery. *Diseases of Aquatic Organisms* **86**, 163-167.
907 **Soldo, A.T. and Merlin, E.J.** (1972). The cultivation of symbiont-free marine ciliates
908 in axenic medium. *The Journal of Protozoology* **19**, 519-524.
909 **Song, W.B. and Wilbert, N.** (2000). Redefinition and redescription of some marine
910 scuticociliates from China, with report of a new species, *Metanophrys siensis*
911 nov. Spec. (Ciliophora, Scuticociliatida). *Zoologischer Anzeiger* **239**, 45-74.

Song, J.Y., Kitamura, S., Oh, M.J., Kang, H.S., Lee, J.H., Tanaka, S.J., and Jung, S.J. (2009a). Pathogenicity of *Miamiensis avidus* (syn. *Philasterides dicentrarchi*), *Pseudocohnilembus persalinus*, *Pseudocohnilembus hargisi* and *Uronema marinum* (Ciliophora, Scuticociliatida). *Diseases of Aquatic Organisms* **83**, 133-143.

Song, J.Y., Sasaki, K., Okada, T., Sakashita, M., Kawahami, H., Matsuoka, S., Kan, H.S., Nakayama, K., Jung, S.J., Oh, M.J. and Kitamura, S.I. (2009b). Antigenic differences of the scuticociliate *Miamiensis avidus* from Japan. *Journal of Fish Disesases* **32**, 1027-1034.

Stidworthy, M.F., Garner, M.M., Bradway, D.S., Westfall, B.D., Joseph, B., Repetto, S., Guglielmi, E., Schmidt-Posthaus, H. and Thornton, S.M. (2014). Nondomestic, exotic, wildlife and zoo animals systemic scuticociliatosis (*Philasterides dicentrarchi*) in sharks. *Veterinary Pathology* **51**, 628-663.

Stoeck, T., Welter, H., Seitz-Bender, D., Kusch, J.and Schmidt, H.J. (2000). ARDRA and RAPD-fingerprint reject the sibling species concept for the ciliate *Paramecium caudatum* (Ciliophora, Protoctista). *Zoologica Scripta* **29**, 75-82.

Thompson, J.C., and Moewus, L. (1964). *Miamiensis avidus* n. g., n. sp., a marine facultative parasite in the ciliate order Hymenostomatida. *The Journal of Protozoology* **11,** 378-381.

Umehara, A., Kosuga, Y. and Hirose, H. (2003). Scuticociliata infection in the weedy sea dragon *Phyllopteryx taeniolatus. Parasitology International* **52**, 165-168.

Whang, I., Kang, H.S. and Lee, J. (2013). Identification of scuticociliates (*Pseudocohnilembus persalinus*, *P. longisetus*, *Uronema marinum* and *Miamiensis avidus*) based on the cox1 sequence. *Parasitology International* **62**, 7-13.

Figures and Table legends

Figure 1. *Paralichthys adspersus:* clinical signs of infection. (A) Visible changes are observed in the pigmentation of infected fish, and (B) the presence of haemorrhagic lesions on the gills. (C) Ciliates obtained from ascites liquid. Histopathological findings of the infection by scuticociliates: (D) Histological section of gills showing the presence of ciliates (arrows), and (E) microphotograph showing a massive infection of ciliates in the myocardium (arrows) causing intense cardiac muscle histophagy. Staining H&E, scale bar = 50 μM.

Figure 2. Morphological characteristics of isolates Pe5 and Pe7 from farmed flounder *Paralichthys adspersus* in comparison with those of *Miamiensis avidus* strain Ma/2 (ATCC® 50180™). Silver carbonate-impregnated trophozoites: isolate Pe5 (A,B); isolate Pe7 (F, G); and *Miamiensis avidus* strain Ma/2 (ATCC® 50180™) (J, M, N). (A, F) Light micrographs showing the oral ciliature and the posterior cell portions (B,G) of isolates Pe5 and Pe7, respectively. (C, D, H) Schematic drawings of the buccal apparatus in *Philasterides dicentrarchi* from sea bass (C), Pe5 (D), and Pe5 (H), showing three oral polykinetids, (M1, M2 and M3) and two paraoral membrane (PM1 and PM2) (E, I) Drawings of posterior ends of isolates Pe5 and Pe7 showing 12 kineties (1-12), the pore of the subterminal contractile vacuole (VP), and a prominent caudal cilium (C, circle). (J) Light microphotograph of silver carbonate-impregned specimens of *M. avidus* strain Ma/2 showing the buccal apparatus. (K, L) Drawings of oral ciliature in *M. avidus* from original description (K) and strain Ma/2 (L) showing the oral polykinetids M1, M2 and M3, and the paraoral membrane (PM). (M) Microphotograph of a trophozoite of *M. avidus* strain Ma/2 showing the spine-

962 shaped apical cell portion (arrow). (N, O) Tomites of *M. avidus* strain Ma/2
963 stained with silver-carbonate (N), and *in vivo* under phase contrast optics (O).
964 Scale bars = 10 μm.

965 **Figure 3**. Structure of nuclear apparatus. Confocal microscope photomicrographs (A, B,
966 D) of trophozoites stained with DAPI, and ligh micrographas of cells stained
967 with silver carbonate (C), showing the position of the macronucleus (M) and
968 micronucleus (m): (A) strain I1 of *Philasterides dicentarchi*, (B) isolate Pe5, (C)
969 isolate Pe7, and (D) strain Ma/2 of *Miamiensis avidus*. Figure C also shows the
970 caudal cilium (c) and the posterior contractile vacuole (cv). Scale bars = 10 μm.

971 **Figure 4.** Induction of tomitogenesis in *M. avidus* and *P. dicentrarchi* under conditions
972 of starvation. Cultures of *M. avidus* (A, B) and *P. dicentrarchi* (C, D), in media
973 with nutrients (A, C) and without nutrients in non-nutrient artificial seawater (B,
974 D). M: macrostomes; m: microstomes; t: tomites. Scale bar = 10 μm.

975 **Figure 5.** (A) Prey-induced transformation of *M. avidus* ATCC® 50180™ (strain Ma/2)
976 co-cultivated with the I1 strain from *Philasterides dicentrarchi* in non-nutrient
977 artificial seawater (NSS). (A-D) Macrostome formation at day 2 of co-cultures
978 showing ciliates ingested in its interior (circles and arrows). (A) Silver staining,
979 (B) phase contrast, (C) acridine orange staining, (D) DAPI staining. (E)
980 Polymerase chain reaction from genomic DNA of *M. avidus* (M), *P.*
981 *dicentrarchi* strain I1 (I1), and *M. avidus* and *P.dicentrarchi* (M+I1) co-
982 cultivated for five days. (F) Primers designed from the nucleotide sequences of *P.*
983 *dicentrarchi* corresponding to (a) the α-tubulin, (b) β-tubulin and (c) the small
984 rRNA subunit (SSUrRNA) gene used for PCR. Mw: molecular size markers.

985 **Figure 6.** Virulence of the Ma / 2 strain of *M. avidus* ATCC® 50180™ in
986 experimentally infected turbot. (A) Abdominal distension due to accumulation

of ascitic fluid in the body cavity. The arrow indicates anal inflammation. (B) Kinetics of cumulative mortality induced after intraperitoneal injection with *M. avidus* five after infection.

Figure 7. Neighbour-joining (NJ) unrooted trees inferred from: SSUrRNA (A), as well as, the α- (B), and β-tubulin (C) nucleotide sequences showing the phylogenetic relationships between isolates Pe5 and Pe7 from the fine flounder, strain I1 of *Philasterides dicentrarchi* isolated from turbot, and strain Ma/2 of *Miamiensis avidus* ATCC® 50180™. The phylogeny was also inferred by analysis of SSUrRNA gene sequences between the isolates from the fine flounder, strains of *Philsterides* isolated from turbot, strains of *Miamiensis* isolated from olive flounder (strains YK2 and YS2), isolate FXP2009050602 of *M. avidus,* and several species of philasterids (see Table 1) including strain GF200806601 of *Philasterides armatalis* (A). Nodes represent bootstrap values of 1000 resampled values in the NJ analysis with the Kimura two-parameter correction model, and the scale bar indicates the genetic distance.

Figure 8. Analysis of the antigenic relationships related to the alpha subunit of tubulin, using a gene fragment (A) between isolates from the fine flounder *P. adspersus*, *Philasterides dicentarchi* strain I1 and *Miamiensis avidus* strain Ma/2 (ATCC® 50180™), by various immunoassays using antibodies generated against a fragment of recombinant α-tubulin. Immunopattern recognition by immunofluorescence: (B) vs. *P. dicentrarchi* strain I1 (confocal microscope image using a combined DAPI staining and staining with FITC), (C) vs. the Pe5 isolate (D) and the Pe7 isolate from the fine flounder *P. adspersus* and, (E) vs. *M. avidus* strain Ma/2. (F) ELISA of the degree of cross-reactivity between α-tubulin from *P. dicentrarchi* strain I1, isolate Pe7 from the fine flounder *P.*

adspersus and *M. avidus* strain Ma/2. The results are expressed as mean values of the absorbance at 492 nm ± standard error (n=5), and asterisks indicate the statistical significance (P <0.01). (G) Western blot analysis of ciliary proteins of *M. avidus* strain Ma/2 (lane 1), *P. dicentrachi* strain I1 (lane 2) and the Pe7 isolate from *P. adspersus* showing two bands of recognition corresponding to two polypeptide fragments of α-tubulin (arrows). Mw: molecular weight markers expressed in kD.

Table 1. List of philasterid species included in the phylogenetic analysis, showing the GenBank Accession numbers for their SSUrRNA gene sequences, the isolates/strains, host specificity, and sequence length in base pairs (bp).

Table 2. Biometric data for silver-impregnated ciliates isolates (Pe5 and Pe7) from *Paralichthys adspersus*, *Philasterides dicentrarchi* strain I1 isolated from turbot, *P. dicentarchi* (Dragesco et al., 1995) from seabass, strains T5 and T16 of *Miamiensis avidus* (Thompson and Moewus 1964), and strain Ma/2 of *M. avidus* (ATCC® 50180™). *Biometric values obtained from specimens of *M. avidus* supplied by ATCC and cultured in our laboratory. †Data obtained from microstomes. The values shown are expressed (in μm) as mean ± standard error, with the minimum-maximum ranges in parentheses. M1-M3: oral polykinetids, PM: paroral membrane; PM1, PM2: paroral membranes 1 and 2. CVP: contractile vacuole pore; Kn: kinety. The measurements were made in 50 specimens. (-) No data available.

Table 3. Nucleotide identity percentage analyzed by the BLAST alignment program between regions of DNA gene of the small subunit of (A) rRNA (SSUrRNA) and (B) α- and β-subunits of tubulin of isolates Pe5 and Pe7 from the fine flounder *Paralichthys adspersus,* strain I1 of *Philasterides dicentrarchi* isolated

from turbot and strain Ma/2 of *Miamiensis avidus* held in ATCC® 50180™. Additionally, the BLAST analysis of the SSUrRNA sequences included the strains YK2 and YS2 of *Miamiensis avidus* isolated from *Paralichthys olivaceus*, and the GF2008082801 strain of *Philasterides armatalis*.

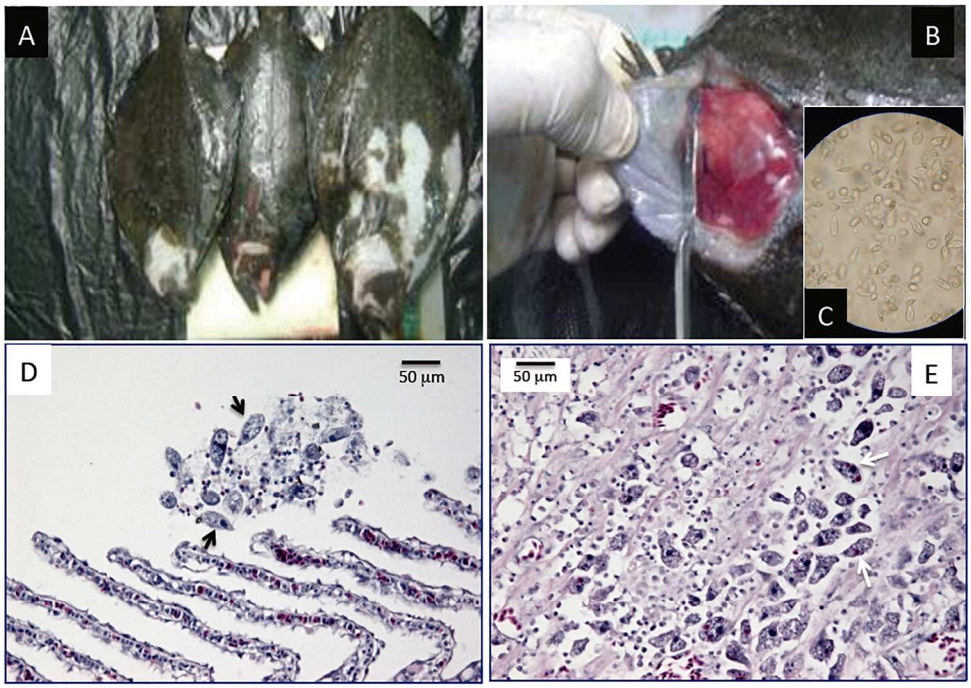

Figure 1

209x150mm (300 x 300 DPI)

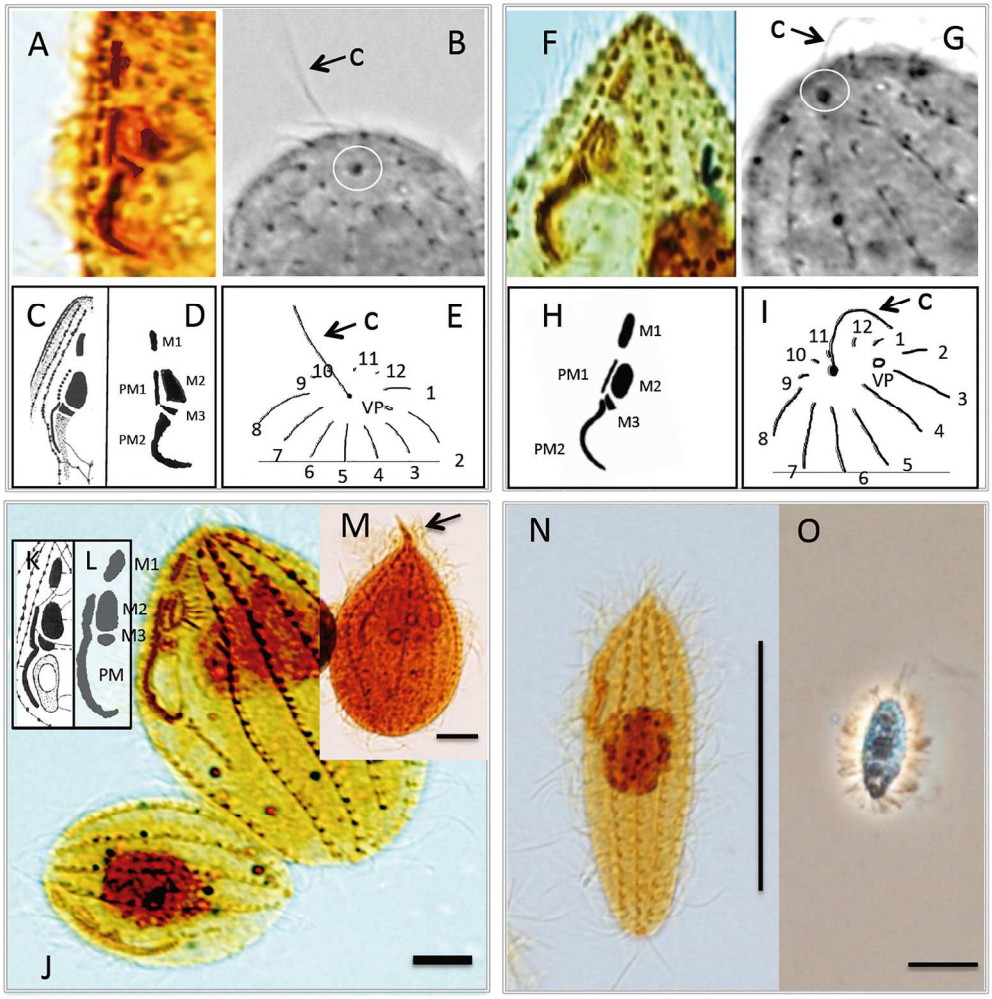

Figure 2

209x214mm (300 x 300 DPI)

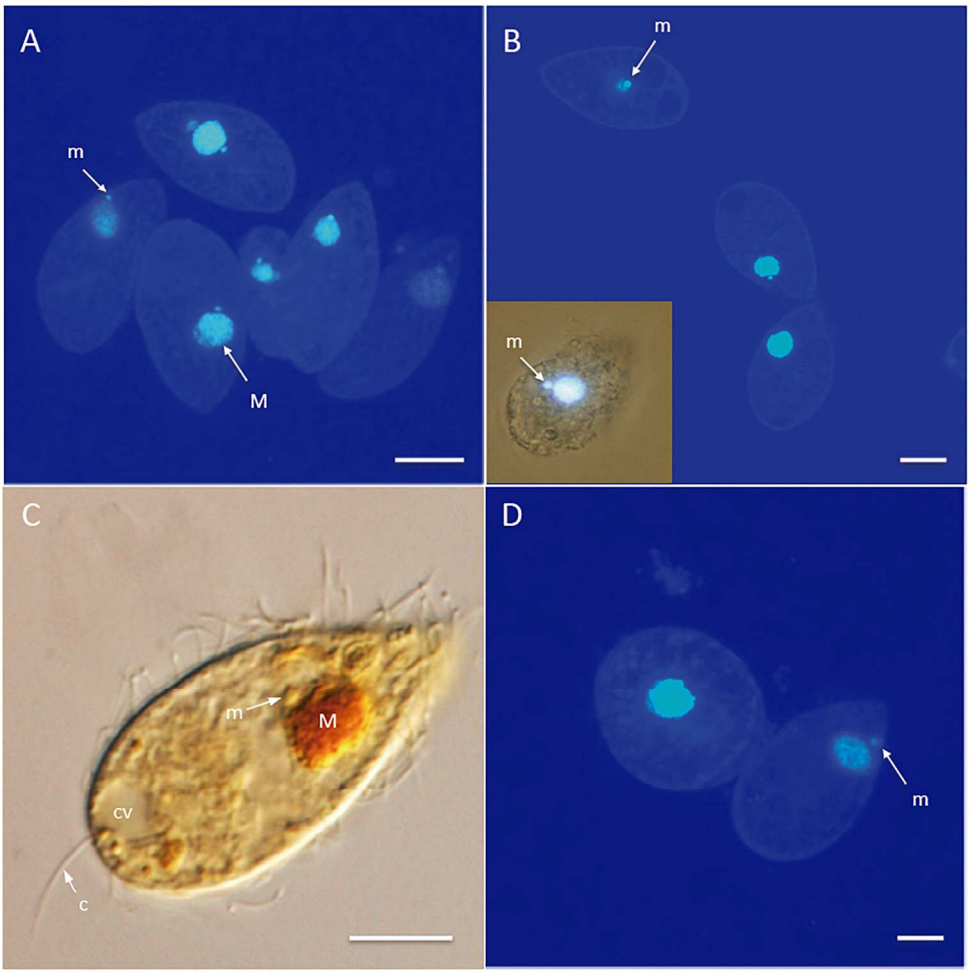

Figure 3

209x210mm (300 x 300 DPI)

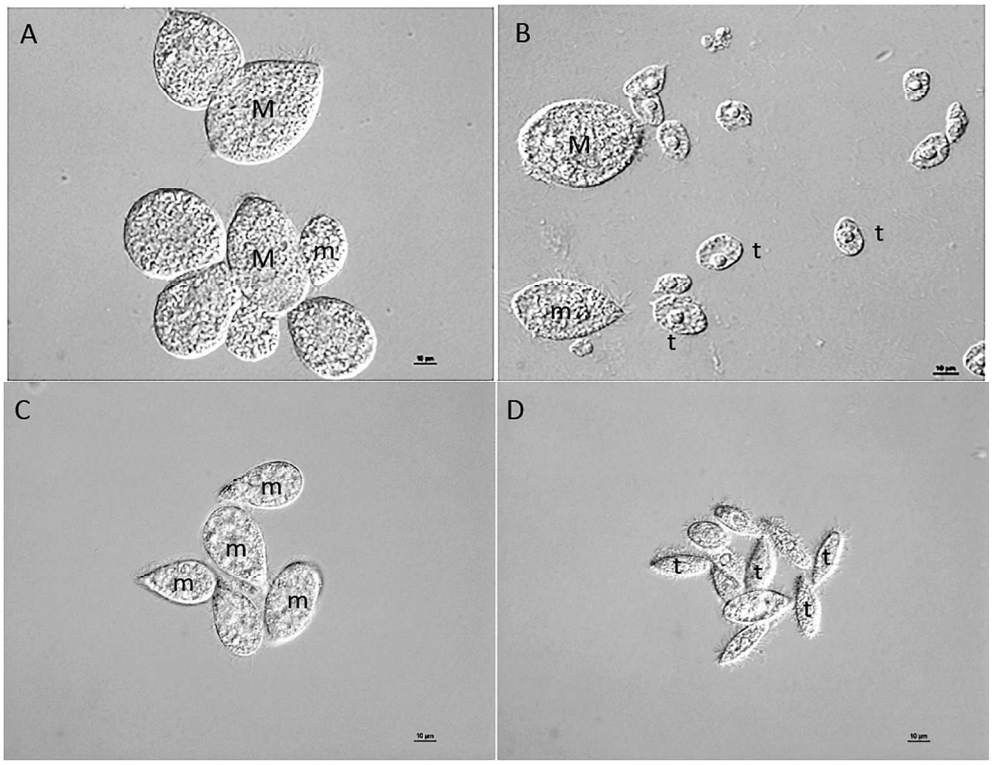

Figure 4

209x162mm (300 x 300 DPI)

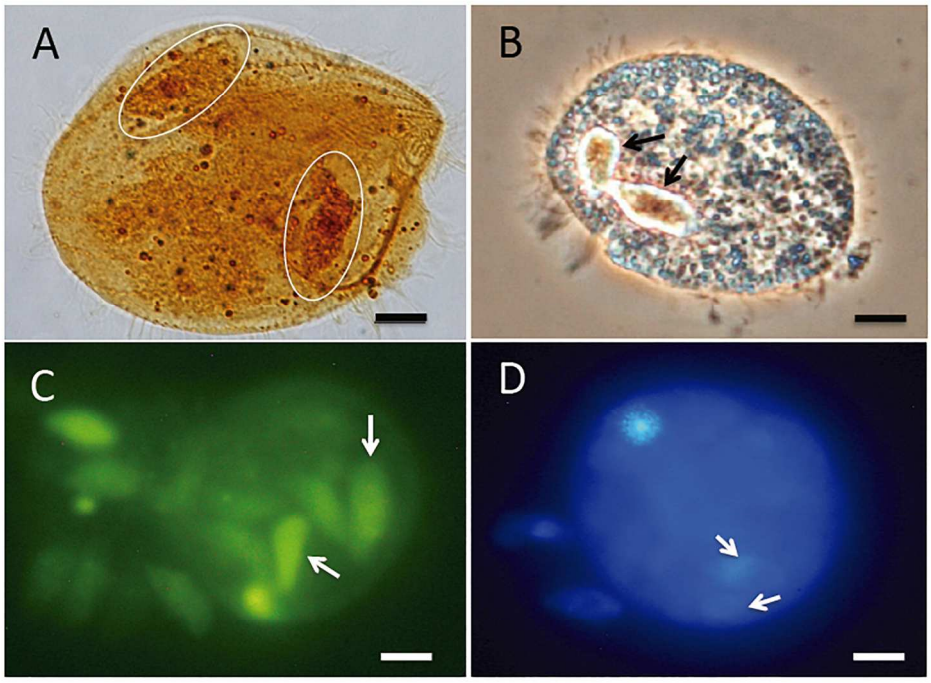

E)

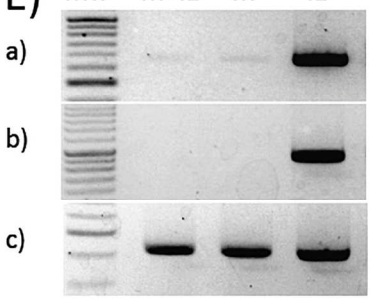

F)

Gene	Sequence forward/reverse (5'-3')	Size fragment (bp)
α-tubulin	TTTAGAACCCACCGTTATTGA TGATTCTGTCTAAGCATAA	161
β-tubulin	CAATAAGGTTCCCATTCC TAATTAATAAAAAATAATTCA	259
SSUrRNA	GAGAAACGGCTACCACATCTA CAGGTAAAGAGCCTACTCCA	349

Figure 5

209x220mm (300 x 300 DPI)

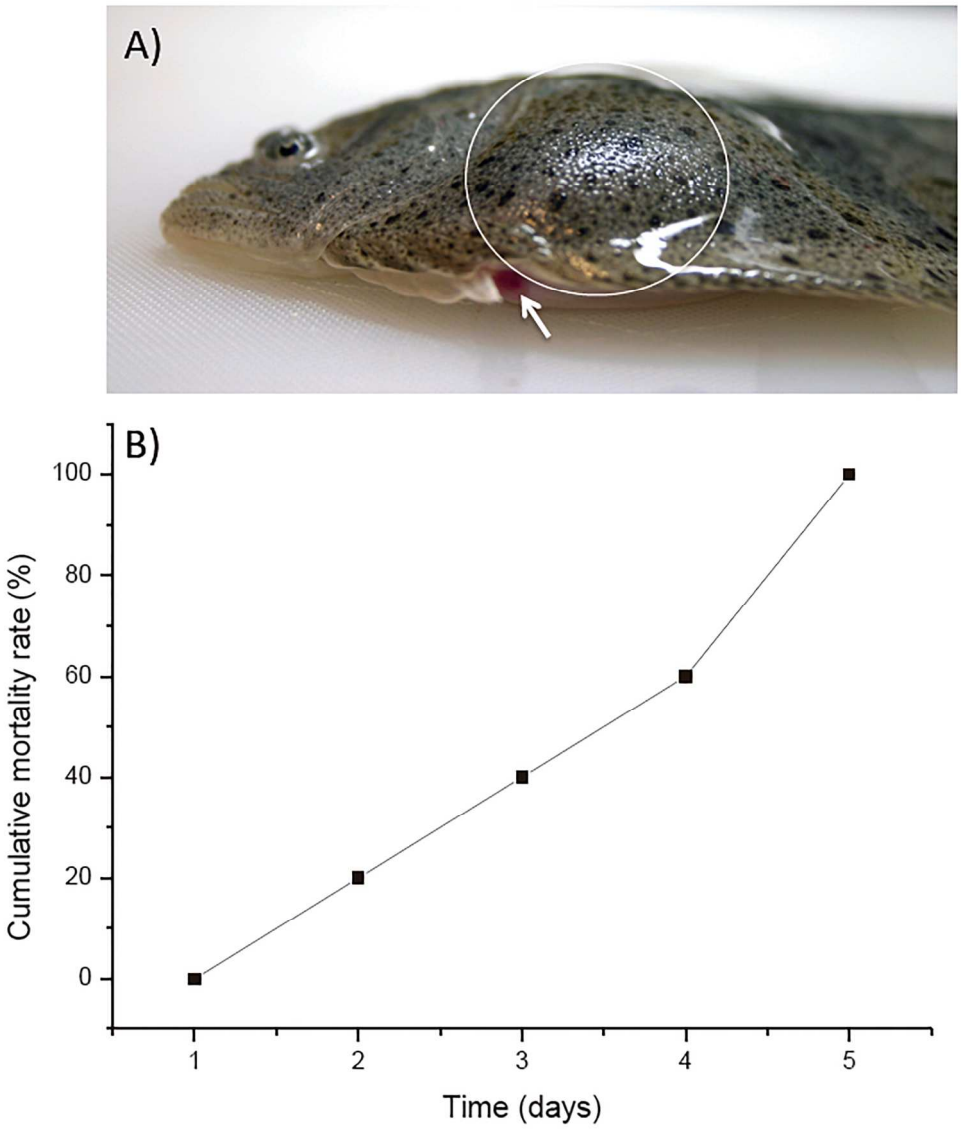

Figure 6

209x242mm (300 x 300 DPI)

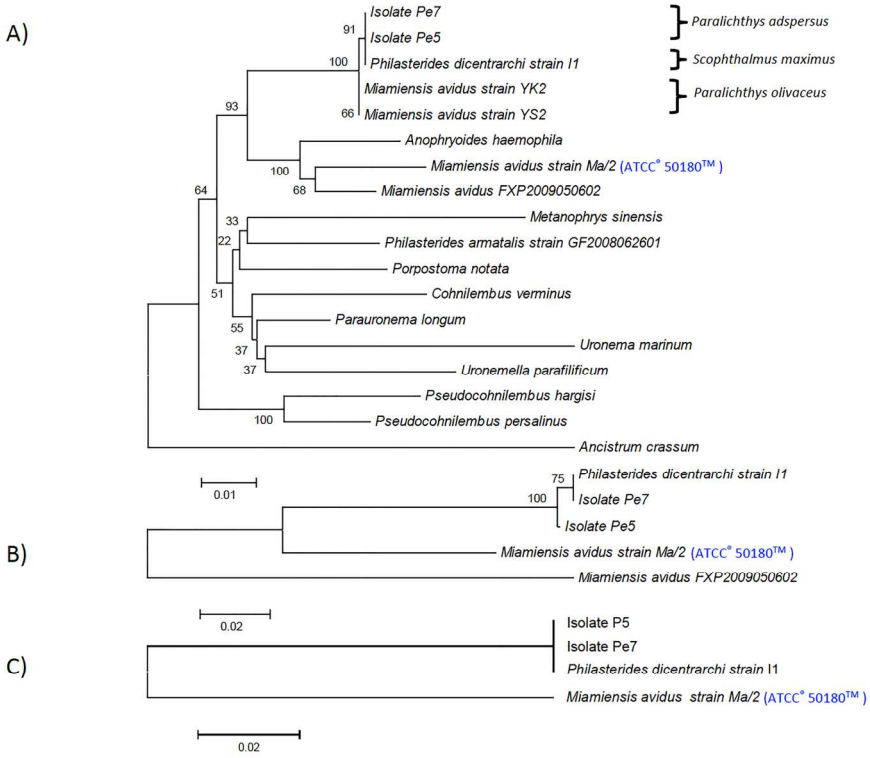

Figure 7

167x133mm (300 x 300 DPI)

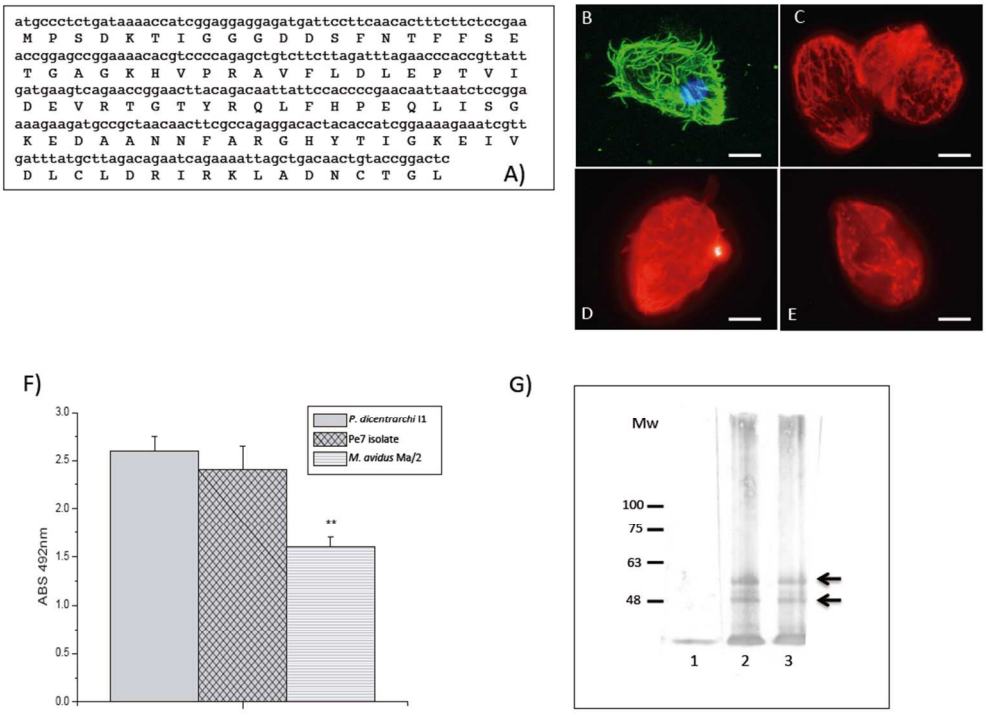

Figure 8

87x64mm (300 x 300 DPI)

Species	Accession number	Isolate/strain	Host	Size (bp)
Ancistrum crassum	HM236340	FXP2009051101	-	1753
Anophryoides haemophila	U51554.1	-	Lobster, *Homarus americanus*	1763
Metanophrys sinensis	HM236336	FXP2009052901	-	1554
Miamiensis avidus ATCC® 50180™	KX357144	Ma/2	Seahorses	1759
Miamiensis avidus	EU831208	YK2	Olive flounder, *Paralichthys olivaceus*	1759
Miamiensis avidus	EU831200	YS2	Olive flounder, *Paralichthys olivaceus*	1759
Miamiensis avidus	JN885091.1	FXP2009050602	-	1760
Parauronema longum	HM236338	FXP200903150	-	1759
Philasterides dicentrarchi	JX914665	I1	Turbot, *Scophthalmus maximus*	1759
Philasterides armatalis	FJ848877	GF2008062601	-	1758
Porpostoma notata	HM236335	FXP2009050601	Seahorses, *Hippocampus hippocampus*	1755
Pseudocohnilembus hargisi	AY833087	SCL-B	Olive flounder, *Paralichthys olivaceus*	1752
Pseudocohnilembus persalinus	AY835669	SCL-A	Olive flounder, *Paralichthys olivaceus*	1754
Uronema marinum	GQ465466	PHB090219	Marine fishes	1758
Uronemella parafilificum	HM236337	FXP2009053001	-	1756

Characteristics	Pe5 isolate	Pe7 isolate	*Philasterides dicentrarchi* strain I1	*Philasterides dicentrarchi*	*Miamiensis avidus*		*Miamiensis avidus strain Ma/2**
Body dimensions							
Length †	39.5 ± 4.5 (25-48)	34.6 ± 5.9 (25-51)	33.6 ± 4.2 (25-43)	35.1 ± 4.8 (23-43)	31.9	39.9	40.2 ± 4.2 (34-46)
Width †	21.5 ± 3.7 (16-28)	19.6 ± 3.8 (12-29)	19.5 ± 3.0 (15-28)	18.5 ± 2.5 (12-25)	16.1	20.1	23.4 ± 2.6 (18-28)
Size of nuclei							
Macronucleus	5.4 ± 0.8 (4-6)	5.9 ± 1.2 (3-8)	7.0 ± 1.0 (5-9)	6.4 ± 1.1 (4-8)	4.1	5.1	13.2 ± 2.6 (6-17)
Micronucleus	1.0 ± 0.2 (0.6-1.2)	1.2 ± 0.3 (0.7-1.6)	1.6 ± 0.2 (1.3-1.9)	1.5 ± 0.2 (1.2-1.8)	Exist	Exist	1.7 ± 0.3 (1.4-2.0)
Somatic cilia							
Total no. of kineties	10-12	10-13	13-14	14 (13-15)	10-12	10-13	9-11
Oral ciliature							
Dist. from apex to M1	3.0 ± 1.1 (1.6-4.3)	3.5 ± 0.6 (3.03-4.6)	3.9 ± 0.5 (2.5-5.0)	3.7 ± 0.7 (3-5)	3-4	3-4	3.3 ± 1.9 (1.4-10.9)
Length of buccal field	14.4 ± 2.4 (9.2-17.6)	12.8 ± 2.2 (8.6-18.3)	18.8 ± 1.3 (15.3-22.1)	-	13.6	17.1	17.7 ± 3.1 (8.9-23.9)
Lenght of PM1	3.2 ± 0.5 (2.4-3.9)	3.1 ± 1.3 (2.2-4.3)	3.7 ± 0.5 (2.5-4.8)	4.1 ± 0.5 (3.5-5)	7.5	9.9	12.7 ± 3.1 (6.9-18.5)
					Sometimes a narrow gap	Sometimes a narrow gap	(continous)
Length of PM2	8.1 ± 7.9 (4.4-10.2)	5.9 ± 1.2 (2.2-7.8)	6.25 ± 1.6 (4.6-7.9)	6.0 ± 1.0 (4.5-8)	-	-	-
Length M1	1.2 ± 0.4 (0.9-1.5)	1.6 ± 0.3 (0.9-1.8)	2.0 ± 1.2 (2.0-2.9)	2.3 ± 0.3 (2-3)	2.6	3	2.75 ± 0.7 (1.4-3.8)
Length M2	1.6 ± 0.3 (1.2-2.1)	1.8 ± 0.4 (1.2-2.4)	3.1 ± 1.8 (2.7-3.5)	2.9 ± 0.4 (2-4)	2.8	3.6	3.5-0.9 (1.3-4.9)
Length M3	0.5 ± 0.2 (0.2-0.9)	0.4 ± 0.1 (0.3-0.7)	0.8 ± 0.5 (0.7-1.0)	1.8±0.3 (1.2-2.1)	1.1	1	1.5±0.4 (0.6-2.3)
Buccal field/Body legth	0.4 ± 0.1 (0.3-0.5)	0.4 ± 0.1 (0.3-0.5)	0.4 ± 0.1 (0.4-0,5)	-	0.4	0.4	0.4 ± 0.1 (0.35-0.55)
Position of CVP	Posterior end of kinety 2	Posterior end of kinety 2	Posterior end of kinety 2	Between kinety 1 & 2	Posterior end of kinety 2 (ocassionally 2 CVP's at the base of kinety 2 and 3)		Posterior end of kinety 2
Characteristics of Kn	Terminate at M1	Terminate at M1	Terminate at M1	Terminate at M1	Terminate at M1		Terminate at M1
Sample location	Huarmey, Perú	Huarmey, Perú	Galicia, Spain	Montpellier, France	Miami, U.S.A.		Miami, USA
Host	*Paralichthys adspersus*	*Paralichthys adspersus*	*Scophthalmus maximus*	*Dicentrarchus labrax*	Sea horses?-local bay waters of Miami, Florida-		Sea horses
Life cycle	Microstome/tomite	Microstome/tomite	Microstome/tomite	-	-		Macrostome/microstome/tomite
Data source	Present study	Present study	Present study	Dragesco et al. (1995)	Thompson & Moewus (1964)		Present study

	M. avidus strain Ma/2	*P. dicentrarchi* isolate Pe5	*P. dicentrarchi* isolate Pe7	*P. dicentrarchi* strain I1	*M. avidus* strain YK2	*P. armatalis* strain GF2008082801
5	96%					
e7	96%	100%				
	96%	100%	100%			95%
	96%	99%	99%	99%		95%
	96%	99%	99%	99%	99%	95%
02	97%	96%	96%	96%	96%	95%

	M. avidus strain Ma/2	*P. dicentrarchi* isolate Pe5	*P. dicentrarchi* isolate Pe7	*P. dicentrarchi* strain I1
e Pe5	α= 89% β= 85%			
e Pe7	α= 89% β= 85%	α= 99% β= 100%		
I1	α= 89% β= 85%	α= 99% β= 99%	α= 100% β= 99%	
50602	α= 83%	α= 82%	α= 81%	α= 81%

Supplementary Material: nucleotide sequences used

Specie	strain	gene	Accession number	Nucleotide sequence	Length (bp)
Philasterides dicentrarchi	I1	18S ribosomal RNA gene, complete sequence	JX914665.1	AATCTGGTTGATCCTGCCAGTAGTCATATGCTTGTCTCAAAGATTAAGCCATGCATGTCTAAGTATAAATAGTATACAGTGAAACT GCGAATGGCTCATTAAAACAGTTATAGTTTATTTGATAATGGAAAGCTACATGGATAACCGTGGTAATTCTAGAGCTAATACATGC TGTCAAACCCGACCTTTGGAAGGGTTGTATTTATTAGATATTAAGCCAATATTCCTTCGGGTCTATTGTGGTGAATCATAGTAACT GATCGAATCTCTTCACGAGATAAATCATTCAAGTTTCTGCCCTATCAGCTTTCGATGGTAGTGTATTGGACTACCATGGCAGTCAC GGGTAACGGAGAATTAGGGTTCGGTTCCGGAGAGGGAGCCTGAGAAACGGCTACCACATCTAAGGAAGGCAGCAGGCGCGTA AATTACCCAATCCTGATTCAGGGAGGTAGTGACAAGAAATAACAACCTGGGGGCCTCACGGCCTTACGGGATTGTAATGAGAAC AATTTAAACGACTTAACGAGGAACAATTGGAGGGCAAGTCTGGTGCCAGCAGCCGCGGTAATTCCAGCTCCAATAGCGTATATT AAAGTTGTTGCAGTTAAAAAGCTCGTAGTTGAACTTCTGCATGTGCCCAGTTCTGGCTTCGGTCAAGCTGTGGTGTATGCATCCG CTTGCAAAGCTAGACCGGTCTTCATTGATCGACTAGTGGAGTAGGCTCTTTACCTTGAAAAAATTAGAGTGTTTCAGGCAGGCAA TGGCTCGAATACATTAGCATGGAATAATGGAATAGGACTTTTGTCCATTTGGTTGGTTATTGGACATAAGTAATGATTAAAAGGGA CAGTTGGGGGCATTAGTATTTAATTGTCAGAGGTGAAATTCTTGGATTTATTAAAGACTAACTTATGCGAAAGCATTTGCCAAGGA TGTTTTCATTAATCAAGAACGAAAGTTAGGGGATCAAAGACGATCAGATACCGTCCTAGTCTTAACTATAAACTATACCGACTCGG AATCGGACCGGCTTATAAAACTGGTTCGGCGCCGTATGAGAAATCAAAGTCTTTGGGTTCTGGGGGGAGTATGGTCGCAAGGCT GAAACTTAAAGGAATTGACGGAAGGGCACCACCAGGCGTGGAGCCTGCGGCTTAATTTGACTCAACACGGGGAAACTTACCAG GTCCAAACATGGGTGGGATTGACAGATTGAGAGCTCTTTCTTGATTCTATGGGTGGTGGTGCATGGCCGTTCTTAGTTGGTGGA GTGATTTGTCTGGTTAATTCCGTTAACGAACGAGACCTTAACCTGCTAAATAGTACGTTGATGCACAATTGGCGTTACTTCTTAGA GGGACTATGCGCTTTGAAACGCATGGAAGTTTGAGGCAATAACAGGTCTGTGATGCCCTTAGATGTCCTGGGCCGCACGCGCG CTACAATGACTCGCTCAGAAAGTACTTCCTGGTCCGGAAGGATTCGGGTAATCTTTTAAATACGAGTCGTGTTAGGGATCGATCT TTGTAATTATGGATCTTGAACGAGGAATGCCTAGTAAGTGCAAGTCATCAGCTTGTACTGATTACGTCCCTGCCCTTTGTACACA CCGCCCGTCGCTCCTACCGATTTCGAGTGATCCGGTGAACCTTCTGGACTGAGCACGCTTGCGTGAACGGGAAGTTAAGTAAAC CTAATCACTTAGAGGAAGGAGAAGTCGTAACAAGGTTTCCGTAGGTGAACCTGCGGAAGGATC	1759
Miamiensis avidus ATCC® 50180™	Ma/2	18S ribosomal RNA gene, complete sequence	KX357144	AATCTGGTTGATCCTGCCAGTAGTCATATGCTTGTCTCAAAGATTAAGCCATGCATGTCTAAGTATAAATAGTATACAGTGAAACT GCGAATGGCTCATTAAAACAGTTATAGTTTATTTGATAATGGAAAGCTACATGGATAACCGTGGTAATTCTAGAGCTAATACATGC TGTTAAGCCTGACTTTTTGGGAGGGCTGTATTTATTAGATATTAAAGCCAATATTCCTTGTGTCTATTGTGGTGAATCATAGTAACT GATCGAATCTCTTTTTTGAGATAAATCATTCAAGTTTCTGCCCTATCAGCTTTCGATGGTAGTGTATTGGACTACCATGGCAGTTAC GGGTAACGGAGAATTAGGGTTCGGTTCCGGAGAGGGAGCCTGAGAAACGGCTACCACATCTAAGGAAGGCAGCAGGCGCGTA AATTACCCAATCCTGATTCAGGGAGGTAGTGACAAGAAATAACAACCTGGGGGACTTTGTCCTTACGGGATTGCAATGAGAACAA TTTAAACGACTTATCGAGGAACAATTGGAGGGCAAGTCTGGTGCCAGCAGCCGCGGTAATTCCAGCTCCAATAGCGTATATTAA AGTTGTTGCAGTTAAAAAGCTCGTAGTTGAATTTCTGTACATGACTGGTTCTGGCCTCGGTCAAGCCTGTTCGTGTGCATCCGCT TGCAAACTGGGACCGGTATTCATTTATCGACCCAGGGAGTAGGCCCTTTACCTTGAAAAAATTAGAGTGTTTCAGGCAGGCAATT GCTCGAATACATTAGCATGGAATAATAGAATAGGACTTTTGTCCATTTGGTTGGTTATTGGACATGAGTAATGATTAAAAGGGACA GTTGGGGGCATTAGTATTTAATTGTCAGAGGTGAAATTCTTGGATTTATTAAAGACTAACTTATGCGAAAGCATTTGCCAAGGATG TTTTCATTAATCAAGAACGAAAGTTAGGGGATCAAAGACGATCAGATACCGTCCTAGTCTTAACTATAAACTATACCGACTCGGAA TCGGGCAGGCTAATAAATCTTGCTCGGCGCCGTATGAAAATCAAAGTCTTTGGGTTCTGGGGGGAGTATGGTCGCAAGGCTGAA ACTTAAAGGAATTGACGGAAGGGCACCACCAGGCGTGGAGCCTGCGGCTTAATTTGACTCAACACGGGGAAACTTACCAGGTC CAAACATGGGTGGGATTGACAGATTGAGAGCTCTTTCTTGATTCTATGGGTGGTGGTGCATGGCCGTTCTTAGTTGGTGGAGTG ATTTGTCTGGTTAATTCCGTTAACGAACGAGACCTTAACCTGCTAAATAGTAGCCTTATGAACAATGGGGTTTACTTCTTAGAGGG ACTATGCGTTTTGAATCGCATGGAAGTTTGAGGCAATAACAGGTCTGTGATGCCCTTAGATGTCCTGGGCCGCACGCGCGCTAC AATGATTCGCTCAGAAAGTATTTCCTGGCCCGGAAGGGTTCAGGGTAATCTTTTCAATACGAATCGTGTTAGGGATCGATCTTTG CAATTATAGATCTTGAACGAGGAATGCCTAGTAAGTGCAAGTCATCAGCTTGTACTGATTACGTCCCTGCCCTTTGTACACACCG CCCGTCGCTCCTACCGATTTCGAGTGATCCGGTGAACCTTCTGGACCGAGAGCGCTTGCGCTCATGGGAAGTTAAGTAAACCTA ATCACTTAGAGGAAGGAGAAGTCGTAACAAGGTTTCCGTAG GTGAACCTGCGGAAGGATC	1759
Isolates Pe5	-	18S ribosomal	-	AATCTGGTTGATCCTGCCAGTAGTCATATGCTTGTCTCAAAGATTAAGCCATGCATGTCTAAGTATAAATAGTATACAGTGAAACT GCGAATGGCTCATTAAAACAGTTATAGTTTATTTGATAATGGAAAGCTACATGGATAACCGTGGTAATTCTAGAGCTAATACATGC	1759

and Pe7		RNA gene, complete sequence		TGTCAAACCCGACCTTTGGAAGGGTTGTATTTATTAGATATTAAGCCAATATTCCTTCGGGTCTATTGTGGTGAATCATAGTAACT GATCGAATCTCTTCACGAGATAAATCATTCAAGTTTCTGCCCTATCAGCTTTCGATGGTAGTGTATTGGACTACCATGGCAGTCAC GGGTAACGGAGAATTAGGGTTCGGTTCCGGAGAGGGAGCCTGAGAAACGGCTACCACATCTAAGGAAGGCAGCAGGCGCGTA AATTACCCAATCCTGATTCAGGGAGGTAGTGACAAGAAATAACAACCTGGGGGCCTCACGGCCTTACGGGATTGTAATGAGAAC AATTTAAACGACTTAACGAGGAACAATTGGAGGGCAAGTCTGGTGCCAGCAGCCGCGGTAATTCCAGCTCCAATAGCGTATATT AAAGTTGTTGCAGTTAAAAAGCTCGTAGTTGAACTTCTGCATGTGCCCAGTTCTGGCTTCGGTCAAGCTGTGGTGTATGCATCCG CTTGCAAAGCTAGACCGGTCTTCATTGATCGACTAGTGGAGTAGGCTCTTTACCTTGAAAAAATTAGAGTGTTTCAGGCAGGCAA TGGCTCGAATACATTAGCATGGAATAATGGAATAGGACTTTTGTCCATTTGGTTGGTTATTGGACATAAGTAATGATTAAAAGGGA CAGTTGGGGGCATTAGTATTTAATTGTCAGAGGTGAAATTCTTGGATTTATTAAAGACTAACTTATGCGAAAGCATTTGCCAAGGA TGTTTTCATTAATCAAGAACGAAAGTTAGGGGATCAAAGACGATCAGATACCGTCCTAGTCTTAACTATAAACTATACCGACTCGG AATCGGACCGGCTTATAAAACTGGTTCGGCGCCGTATGAGAAATCAAAGTCTTTGGGTTCTGGGGGGAGTATGGTCGCAAGGCT GAAACTTAAAGGAATTGACGGAAGGGCACCACCAGGCGTGGAGCCTGCGGCTTAATTTGACTCAACACGGGGAAACTTACCAG GTCCAAACATGGGTGGGATTGACAGATTGAGAGCTCTTTCTTGATTCTATGGGTGGTGGTGCATGGCCGTTCTTAGTTGGTGGA GTGATTTGTCTGGTTAATTCCGTTAACGAACGAGACCTTAACCTGCTAAATAGTACGTTGATGCACAATTGGCGTTACTTCTTAGA GGGACTATGCGCTTTGAAACGCATGGAAGTTTGAGGCAATAACAGGTCTGTGATGCCCTTAGATGTCCTGGGCCGCACGCGCG CTACAATGACTCGCTCAGAAAGTACTTCCTGGTCCGGAAGGATTCGGGTAATCTTTTAAATACGAGTCGTGTTAGGGATCGATCT TTGTAATTATGGATCTTGAACGAGGAATGCCTAGTAAGTGCAAGTCATCAGCTTGTACTGATTACGTCCCTGCCCTTTGTACACA CCGCCCGTCGCTCCTACCGATTTCGAGTGATCCGGTGAACCTTCTGGACTGAGCACGCTTGCGTGAACGGGAAGTTAAGTAAAC CTAATCACTTAGAGGAAGGAGAAGTCGTAACAAGGTTTCCGTAGGTGAACCTGCGGAAGGATC	
Philasterides dicentrarchi	I1	Alpha tubulin, partial sequence	KX357145	TCTTAGATTTAGAACCCACCGTTATTGATGAAGTCAGAACCGGAACTTACAGACAATTATTCCACCCCGAACAATTAATCTCCGGA AAAGAAGATGCCGCTAACAACTTCGCCAGAGGACACTACACCATCGGAAAAGAAATCGTTGATTTATGCTTAGACAGAATCAGAA AATTAGCTGACAACTGTACCGGACTC	197
Miamiensis avidus ATCC® 50180™	Ma/2	Alpha tubulin, partial sequence	KX357143	TCTTAGATCTCGAACCCACCGTTATCGATGAAGTTAGAACCGGAACTTATAGACAACTCTTCCACCCCGAATAATTGATCTCCGG AAAAGAAGATGCCGCCAACAACTTCGCCAGAGGACATTACACTATCGGAAAAGAAATCGTTGACCTTTGTCTCGATAGAATTAGA AAACTCGCTGACAACTGTACCGGATCT	197
Isolate Pe5	-	Alpha tubulin, partial sequence	-	TCTTAGATTTGGAACCCACCGTTATTGATGAAGTCAGAACCGGAACTTACAGACAATTATTCCACCCCGAACAATTAATCTCCGG AAAAGAAGATGCCGCTAACAACTTCGCCAGAGGACACTACACCATCGGAAAAGAAATCGTTGATTTATGCTTAGACAGAATCAGA AAATTAGCTGACAACTGTACCGGACTC	197
Isolate Pe7	-	Alpha tubulin, partial sequence	-	TCTTAGATTTAGAACCCACCGTTATTGATGAAGTCAGAACCGGAACTTACAGACAATTATTCCACCCCGAACAATTAATCTCCGGA AAAGAAGATGCCGCTAACAACTTCGCCAGAGGACACTACACCATCGGAAAAGAAATCGTTGATTTATGCTTAGACAGAATCAGAA AATTAGCTGACAACTGTACCGGACTC	197
Philasterides dicentrarchi	I1	Beta tubulin,	CQ342956.1	CCATAATTCTGTCGGGGGTATTCTTCTCTGACTTTGGAGATCAATAAGGTTCCCATTCCGGATCCAGTTCCTCCTCCTAAAGAGTG GGTGATTTAGAATCCTTATAAGCAATCACATCCTTCAGCTTCTTTTCTGACAACATCTAAAACAGAGTCGATTAATTCAGCTCCTTC GGTGTAGTGTCCTTTGGCCCAGTtGTTACCGGCTCCGGTTTATCCGAAAACGCTATTTAATTATTTAATTTTAATTACATTCTTTCTT CAATATATAAAACAATTATGAATTATTTTTTATTAATTATTACAAGTTATCAGGTCTGAAGAGTTGTCCGAAAGGTCCAGCTCTAAC	388

		partial sequence		GGAATCCATGGTACCGGGTTCCAAATCCATAAGGATGGCTC	
Miamiensis avidus ATCC® 50180™	Ma/2	Beta tubulin, partial sequence	KX357147	CCATAATTCTGTCGGGGTATTCTTCTCTGACTTTGGAGATAAGGAGGGTACCCATTCCGGATCCAGTTCCTCCTCCAAGAGAGTG GGTGATTTAGAAACCTTATAAGCAATCACATCCTTCGGCTTCTTTTCTGACGACATCCAAAACGGAGTCGATCAATTCAGCTCCTT CGGTGTAATGACCTTTGGCCCAGTTGTTACCAGCTCCAGTTTGTCCGAAAACGCTATTATAAAATAAAATTAATATTTTCTCAGTTT TTAATATATTTCAATGTGTATTTACAAGTTATCGGGTCTGAAGAGTTGACCGAAAGGTCCAGCTCTTACGGAATCCATGGTTCCGG GTTCGAGATCCATTAAGATGGCTCTGGGAACGTATCTTCCTCCG	388
Pe5 isolate	-	Beta tubulin, partial sequence	-	CCATAATTCTGTCGGGGTATTCTTCTCTGACTTTGGAGATCAATAAGGTTCCCATTCCGGATCCAGTTCCTCCTCCTAAAGAGTG GGTGATTTAGAATCCTTATAAGCAATCACATCCTTCAGCTTCTTTTCTGACAACATCTAAAACAGAGTCGATTAATTCAGCTCCTTC GGTGTAGTGTCCTTTGGCCCAGTTGTTACCGGCTCCGGTTTATCCGAAAACGCTATTTAATTATTTAATTTTAATTACATTCTTTCT TCATTATATAAAACAATTATGAATTATTTTTTATTAATTATTACAAGTTATCAGGTCTGAAGAGTTGTCCGAAAGGTCCAGCTCTAAC GGAATCCATGGTACCGGGTTCCAAATCCATAAGGATGGCTC	388
Pe7 isolate	-	Beta tubulin, partial sequence	-	CCATAATTCTGTCGGGGTATTCTTCTCTGACTTTGGAGATCAATAAGGTTCCCATTCCGGATCCAGTTCCTCCTCCTAAAGAGTG GGTGATTTAGAATCCTTATAAGCAATCACATCCTTCAGCTTCTTTTCTGACAACATCTAAAACAGAGTCGATTAATTCAGCTCCTTC GGTGTAGTGTCCTTTGGCCCAGTTGTTACCGGCTCCGGTTTATCCGAAAACGCTATTTAATTATTTAATTTTAATTACATTCTTTCT TCATTATATAAAACAATTATGAATTATTTTTTATTAATTATTACAAGTTATCAGGTCTGAAGAGTTGTCCGAAAGGTCCAGCTCTAAC GGAATCCATGGTACCGGGTTCCAAATCCATAAGGATGGCTC	388